

# Follicular helper T cells are required for systemic autoimmunity

Michelle A. Linterman,<sup>1</sup> Robert J. Rigby,<sup>1</sup> Raphael. K. Wong,<sup>1</sup> Di Yu,<sup>1</sup> Robert Brink,<sup>2</sup> Jennifer L. Cannons,<sup>3</sup> Pamela L. Schwartzberg,<sup>3</sup> Matthew C. Cook,<sup>4,6</sup> Giles D. Walters,<sup>5,6</sup> and Carola G. Vinuesa<sup>1</sup>

<sup>1</sup>Division of Immunology and Genetics, The John Curtin School of Medical Research, Australian National University, Canberra, ACT 2601, Australia

<sup>2</sup>Garvan Institute of Medical Research, Sydney, NSW 2010, Australia

<sup>3</sup>National Human Genome Research Institute, National Institutes of Health, Bethesda, MD 20892

<sup>4</sup>Department of Immunology and <sup>5</sup>Department of Renal Medicine, The Canberra Hospital, Canberra, ACT 2605, Australia

<sup>6</sup>Australian National University Medical School, Canberra, ACT 2605, Australia

**Production of high-affinity pathogenic autoantibodies appears to be central to the pathogenesis of lupus. Because normal high-affinity antibodies arise from germinal centers (GCs), aberrant selection of GC B cells, caused by either failure of negative selection or enhanced positive selection by follicular helper T (T<sub>FH</sub>) cells, is a plausible explanation for these autoantibodies. Mice homozygous for the *san* allele of *Roquin*, which encodes a RING-type ubiquitin ligase, develop GCs in the absence of foreign antigen, excessive T<sub>FH</sub> cell numbers, and features of lupus. We postulated a positive selection defect in GCs to account for autoantibodies. We first demonstrate that autoimmunity in *Roquin*<sup>san/san</sup> (*sanroque*) mice is GC dependent: deletion of one allele of *Bcl6* specifically reduces the number of GC cells, ameliorating pathology. We show that *Roquin*<sup>san</sup> acts autonomously to cause accumulation of T<sub>FH</sub> cells. Introduction of a null allele of the signaling lymphocyte activation molecule family adaptor *Sap* into the *sanroque* background resulted in a substantial and selective reduction in *sanroque* T<sub>FH</sub> cells, and abrogated formation of GCs, autoantibody formation, and renal pathology. In contrast, adoptive transfer of *sanroque* T<sub>FH</sub> cells led to spontaneous GC formation. These findings identify T<sub>FH</sub> dysfunction within GCs and aberrant positive selection as a pathway to systemic autoimmunity.**

## CORRESPONDENCE

Carola G Vinuesa:  
carola.vinuesa@anu.edu.au

Abbreviations used: ANA, anti-nuclear antibody; dsDNA, double-stranded DNA; GC, germinal center; H&E, hematoxylin and eosin; HEL, hen egg lysozyme; miRNA, microRNA; SHM, somatic hypermutation; SLE, systemic lupus erythematosus; SRBC, sheep red blood cell; T<sub>FH</sub>, follicular helper T.

Systemic lupus erythematosus (SLE) is the prototypic systemic autoimmune disorder. With highly variable clinical manifestations and only 4 out of 11 criteria required to establish the diagnosis (1), multiple pathogenic pathways are likely to contribute to end-organ damage in this disease. Elucidating the different pathways that lead to lupus in particular subsets of patients and identifying biomarkers that flag the different pathways is essential to design more specific and effective therapies.

The formation of autoantibodies against cell nuclear components, including double-stranded DNA (dsDNA), ribonuclear proteins, and histones, is a consistent feature and therefore likely to be fundamental to the disease. This is supported by the observation that formation of autoantibodies precedes development of clinical manifestations of lupus (2), evidence that some of these antibodies contribute to end-organ damage, and

the efficacy of B cell-depleting therapy with rituximab (3). Identification of defects that result in autoantibody formation is therefore of considerable importance in understanding the pathogenesis of lupus.

Numerous engineered and spontaneous defects in central and peripheral tolerance result in antinuclear antibodies (ANAs). However, the specificity and high affinity of the autoantibody response in lupus points to a defect in the response to self-antigen in the periphery. During T-dependent responses, activated B cells receive help from T cells in the T cell zones of secondary lymphoid tissues, and differentiate either extrafollicularly into short-lived plasma cells that produce low-affinity antibody, or enter the follicular

© 2009 Linterman et al. This article is distributed under the terms of an Attribution-NonCommercial-Share Alike-No Mirror Sites license for the first six months after the publication date (see <http://www.jem.org/misc/terms.shtml>). After six months it is available under a Creative Commons License (Attribution-NonCommercial-Share Alike 3.0 Unported license, as described at <http://creativecommons.org/licenses/by-nc-sa/3.0/>).

pathway and form germinal centers (GCs) (4). Within this microenvironment, B cells undergo somatic hypermutation (SHM) and isotype switching, resulting in the generation of memory B cells and long-lived plasma cells that secrete high-affinity antigen-specific IgG antibodies (5, 6). Selection of mutated high-affinity GC B cells depends on restimulation with antigen arrayed on follicular dendritic cells and provision of help by follicular T helper ( $T_{FH}$ ) cells.

Because SHM has the potential to generate self-reactive antibodies (7), it has been long thought that aberrant selection within GCs represents a candidate pathway to the production of lupus-associated autoantibodies. Indeed, autoantibodies detected in SLE patients and mouse lupus models are generally high affinity and somatically mutated (7, 8). Exclusion of self-reactive B cells from GCs has been shown to be defective in SLE patients. Also, GCs have been shown to form spontaneously in several different mouse models of lupus (9), and these are rich in apoptotic cells displaying the antigenic targets of lupus autoimmunity (10, 11). Although SHM can occur outside GCs, this process is far less efficient (12, 13). Despite all of this circumstantial evidence, there is to date no definite proof that GCs and/or  $T_{FH}$  cells are directly required for the production of lupus autoantibodies or end-organ damage. In contrast, extrafollicular affinity maturation of autoantibodies to dsDNA in MRL<sup>lpr</sup> mice (14, 15) and T-independent B cell activating factor of the TNF family–driven pathways to lupus have been demonstrated (16, 17).

Furthermore, the prevailing model is that within GCs, autoantibodies might arise because of defects in negative rather than positive selection, because GC B cells are programmed to undergo apoptosis by default if they do not receive T cell selection signals. This is consistent with evidence that centrocytes down-regulate apoptosis inhibitors such as Bcl-2 and Bcl-xL while up-regulating proapoptotic molecules such as Fas and Bim (18). Normally, a dedicated population of  $T_{FH}$  cells is thought to provide help during selection of GC B cells (19, 20), and indeed a correlation between increased numbers of  $T_{FH}$  cells and autoimmunity has been described in mouse models of lupus (21, 22), suggesting that defects in positive selection by  $T_{FH}$  cells might indeed lead to lupus. Although recent evidence has suggested that Th17 cells may be responsible for aberrant selection of self-reactive GC B cells and autoantibody formation in BXD2 mice (23), direct evidence that  $T_{FH}$  cells can drive autoimmunity has not been provided.

The *sanroque* strain was discovered from screening an ENU mutagenized mouse library for autoimmune regulators (24), and exhibits a lupus-like phenotype characterized by high-affinity anti-dsDNA antibodies, hypergammaglobulinemia, lymphadenopathy, splenomegaly, autoimmune thrombocytopenia, and glomerulonephritis with IgG-containing immune complex deposits. Both the autoimmunity and cellular characteristics of *sanroque* segregate with homozygosity for the *san* allele (M<sub>199</sub>R substitution) of *Roquin* (*Roquin*<sup>san/san</sup>) (22). *Roquin* has been demonstrated to be a regulator of the stability T cell messenger RNAs. Development of autoimmunity in *Roquin*<sup>san/san</sup> mice also correlates with spontaneous GC formation, which is

largely driven by B cell–extrinsic factors (22). *Roquin*<sup>san/san</sup> mice have a marked accumulation of T cells within the B cell follicles, and the  $T_{FH}$  subset is overrepresented within the CD4<sup>+</sup> cell compartment.

In this paper, we report that dysregulation of the GC response through excessive formation of  $T_{FH}$  cells is responsible for autoimmunity in *Roquin*<sup>san/san</sup> mice. Loss of one allele of *Bcl6*, the master transcriptional regulator of GCs (25, 26), significantly reduces spontaneous GC formation in *Roquin*<sup>san/san</sup> mice and the lupus phenotype. Furthermore, deletion of *Sap* (*Sh2d1a*) from *Roquin*<sup>san/san</sup> mice causes a dramatic reduction of  $T_{FH}$  cells and IL-21. *Sap* is a small adaptor protein necessary for signaling through the signaling lymphocyte activation molecule family cell-surface receptors that regulates signals downstream of the TCR. *Roquin*<sup>san/san</sup> *Sap*<sup>-/-</sup> CD4<sup>+</sup> cells also express lower levels of ICOS than *Roquin*<sup>san/san</sup> *Sap*<sup>+/+</sup> cells. This results in abrogation of ANAs (including anti-dsDNA) and end-stage renal disease. These findings establish a causal pathway from the *san* allele of *Roquin* to excess  $T_{FH}$  formation, aberrant GC formation, and positive selection of pathogenic high-affinity autoantibodies to illuminate a novel pathway of lupus pathogenesis.

## RESULTS

### Heterozygous *Bcl6* deficiency reduces spontaneous GCs and attenuates autoimmunity in *Roquin*<sup>san/san</sup> mice

BCL6 has been shown to be the master transcriptional regulator of GC B cells (27). As BCL6 deficiency results in early mortality because of widespread inflammation, we investigated *Bcl6*<sup>+/-</sup> mice for possible defects in the GC response. 8 d after sheep red blood cell (SRBC) immunization, the percentage of GC cells was more than fivefold lower in mice heterozygous for *Bcl6* deficiency ( $2.3 \pm 0.59\%$  vs.  $0.43 \pm 0.46\%$ ;  $P = 0.0011$ ; Fig. 1 a).

To determine whether *Bcl6* heterozygosity could curtail the spontaneous GC response in *Roquin*<sup>san/san</sup> mice, we compared the percentage of GC cells in unimmunized *Roquin*<sup>san/san</sup> *Bcl6*<sup>+/+</sup> and *Roquin*<sup>san/san</sup> *Bcl6*<sup>+/-</sup> mice. As seen in wild-type mice, loss of one allele of *Bcl6* caused a twofold reduction ( $4.4 \pm 1.9\%$  vs.  $2.1 \pm 0.5\%$ ;  $P = 0.0026$ ) in the percentage of spontaneous GCs in *Roquin*<sup>san/san</sup> mice (Fig. 1 b). Loss of one allele of *Bcl6* also reduced GC B cells after SRBC immunization in a cell-autonomous manner (Fig. S1, available at <http://www.jem.org/cgi/content/full/jem.20081886/DC1>).

We then tested whether reduction in the spontaneous GC response in *Roquin*<sup>san/san</sup> *Bcl6*<sup>+/-</sup> mice was accompanied by reduced pathology. Serum dsDNA antibodies were present in 50% of *Roquin*<sup>san/san</sup> *Bcl6*<sup>+/-</sup> mice tested compared with 100% of *Roquin*<sup>san/san</sup> *Bcl6*<sup>+/+</sup> mice (Fig. 1 c). Kidney pathology was also significantly reduced in *Roquin*<sup>san/san</sup> *Bcl6*<sup>+/-</sup> mice (Fig. 1, d and e).

### The lupus-like pathology of *Roquin*<sup>san/san</sup> mice requires T cell activation

We have previously demonstrated that *Roquin* acts predominantly B cell extrinsically to induce spontaneous GC formation,

and T cell intrinsically to prevent accumulation of activated/memory T cells and repress ICOS expression (22, 28). These findings suggest that the spontaneous GC reaction is driven by Roquin-mediated dysregulation of T cells. In a first attempt to confirm that *Roquin<sup>san/san</sup>* lupus is T cell driven, we generated *Roquin<sup>san/san</sup>* mice deficient in the major T cell co-stimulator CD28 (*Cd28<sup>-/-</sup>* mice). Failure to prime T cells in *Roquin<sup>san/san</sup> Cd28<sup>-/-</sup>* mice abrogated the production of antinuclear IgG, including high-affinity anti-dsDNA antibodies (Fig. 2 a). Both interstitial nephritis and glomerular pathology, characterized by increased mesangial cellularity and dense deposits observed in 6-mo-old *Roquin<sup>san/san</sup>* mice, were substantially reduced in age-matched *Roquin<sup>san/san</sup> Cd28<sup>-/-</sup>* mice, with only very mild interstitial nephritis (Fig. 2, b and c). Less than half of the *Roquin<sup>san/san</sup> Cd28<sup>-/-</sup>* mice examined had low-grade mesangial immune complex deposits (Fig. 2 c). Of note, *Roquin<sup>san/san</sup> Cd28<sup>-/-</sup>* naive CD4<sup>+</sup> T cells had a twofold decrease in ICOS expression (29).

### Expansion of the T<sub>FH</sub> subset in *Roquin<sup>san/san</sup>* mice is T cell intrinsic

We have previously reported the similarity of the gene expression profiles of *Roquin<sup>san/san</sup>* CD4<sup>+</sup> T cells and T<sub>FH</sub> cells. Furthermore, *Roquin<sup>san/san</sup>* T cells accumulate in the splenic GCs (22). To formally assess whether T<sub>FH</sub> cells, defined as CD4<sup>+</sup>CXCR5<sup>+</sup>PD-1<sup>high</sup> (30), are expanded in *Roquin<sup>san/san</sup>* mice, we analyzed the percentage and total number of these cells in unimmunized mice and found more than a threefold increase of this subset in *Roquin<sup>san/san</sup>* mice compared with littermate controls (Fig. 2 d). To determine whether this aberrant T<sub>FH</sub> cell accumulation is cell intrinsic, we generated mixed chimeras. Sublethally irradiated *Roquin<sup>+/+</sup>Ly5<sup>a</sup>* mice were reconstituted with a 1:1 mix of *Roquin<sup>+/+</sup>Ly5<sup>a</sup>* and *Roquin<sup>san/san</sup>Ly5<sup>b</sup>* bone marrow cells. As a control, *Roquin<sup>+/+</sup>Ly5<sup>a</sup>* mice were reconstituted with a 1:1 mix of *Roquin<sup>+/+</sup>Ly5<sup>a</sup>* and *Roquin<sup>+/+</sup>Ly5<sup>b</sup>* bone marrow cells. 8 wk after reconstitution, mice were immunized with SRBCs, and the percentage of T<sub>FH</sub> cells derived from each type of donor marrow was determined by flow cytometry. In chimeras reconstituted with *Roquin<sup>+/+</sup>Ly5<sup>a</sup>/Roquin<sup>san/san</sup>Ly5<sup>b</sup>* marrow, three times more Ly5<sup>b</sup> (*Roquin<sup>san/san</sup>*) T<sub>FH</sub> cells than Ly5<sup>a</sup> cells were observed ( $P = 0.001$ ), whereas in controls, an equivalent proportion of T<sub>FH</sub> cells arose from Ly5<sup>a</sup> and Ly5<sup>b</sup> cells ( $P = 0.56$ ; Fig. 2 e). This indicates that Roquin acts in T cells to repress the formation and/or survival of T<sub>FH</sub> cells. Consistent with the observed increase in T<sub>FH</sub> cell numbers, IL-21 production was more than twofold higher in splenocyte cultures from *Roquin<sup>san/san</sup>* mice (Fig. 2 f).

Although T<sub>FH</sub> cells are expanded in *Roquin<sup>san/san</sup>* mice, it was important to exclude defects in other T cell subsets implicated in autoimmunity. CD4<sup>+</sup>CD25<sup>+</sup>FoxP3<sup>+</sup> T reg cells have been shown to play a role in the regulation of lupus-associated autoantibodies (31). T reg cells are not reduced in number or function in *Roquin<sup>san/san</sup>* mice (22). Quantification of FoxP3<sup>+</sup>CD25<sup>+</sup>CD4<sup>+</sup> cells in the spleen confirmed previous observations: *Roquin<sup>san/san</sup>* mice have approximately twofold more T reg cells than wild-type mice ( $18.9 \pm 3.69\%$  vs.  $9.76 \pm 1.03\%$ , respectively; Fig. S2 a, available at <http://www>

[.jem.org/cgi/content/full/jem.20081886/DC1](http://www.jem.org/cgi/content/full/jem.20081886/DC1)). This argues against a role for reduced T reg cell numbers in driving the T cell-mediated disease of *Roquin<sup>san/san</sup>* mice. Another T helper subset, Th17 cells, have emerged as potent mediators of autoimmunity (31), and recent work suggests that they may be critical to maintain the spontaneous GCs of BXD2 mice (23). To test whether Th17 cell activity is dysregulated in *Roquin<sup>san/san</sup>* mice, we analyzed IL-17 levels in splenocyte cell cultures after activation with PMA and ionomycin. IL-17 was detected at comparable levels in cultures from *Roquin<sup>+/+</sup>* and *Roquin<sup>san/san</sup>* mice (Fig. S2 b). In contrast, IL-21, a cytokine secreted by both T<sub>FH</sub> and Th17 cells (33, 34), was found at significantly higher levels in *Roquin<sup>san/san</sup>* splenocyte cultures (Fig. 2 f). Collectively these data indicate that the T<sub>FH</sub> subset in *Roquin<sup>san/san</sup>* mice is expanded in a cell-autonomous manner, whereas T reg and Th17 cells do not appear to be dysregulated in a way that has been previously described to result in autoimmunity.

### SAP-deficient mice form reduced numbers of T<sub>FH</sub> cells

Having established that Roquin acts T cell intrinsically to dysregulate T<sub>FH</sub> cell numbers leading to the formation of abundant GCs, we hypothesized that disrupting the GC reaction through selective reduction of T<sub>FH</sub> cell numbers or function would attenuate systemic autoimmunity. SAP is an adaptor protein necessary for signaling through the signaling lymphocyte activation molecule family receptors that regulates signals downstream of the TCR. Mice lacking SAP cannot form GCs or generate immunological memory after immunization, a result of impaired CD4<sup>+</sup> T cell help to GC B cells after antigen exposure (35–38). To date, it is not known whether SAP signaling is also required to maintain optimal T<sub>FH</sub> cell numbers. We enumerated CD4<sup>+</sup>CXCR5<sup>+</sup>PD-1<sup>high</sup> T<sub>FH</sub> cells in SAP-deficient unimmunized mice and wild-type littermates, and observed a twofold decrease in the number of basal T<sub>FH</sub> cells (Fig. 3 a, left). This was accompanied by a fourfold reduction in the number of background GC B cells (Fig. 3 b, right).

### *Roquin<sup>san/san</sup> Sap<sup>-/-</sup>* mice do not form excessive T<sub>FH</sub> cells or spontaneous GCs

Once we had established that SAP deficiency not only impairs CD4<sup>+</sup> T cell help for GC B cells but also decreases T<sub>FH</sub> cell numbers, we generated *Roquin<sup>san/san</sup> Sap<sup>-/-</sup>* mice to determine whether numerically and functionally defective T<sub>FH</sub> cells in *Roquin<sup>san/san</sup>* mice could abrogate the spontaneous GC reactions. As observed in SAP-deficient mice, loss of SAP in *Roquin<sup>san/san</sup>* mice also had an effect on T<sub>FH</sub> cell numbers: there was a fourfold reduction ( $0.94 \pm 0.41\%$  vs.  $3.59 \pm 1.99\%$ ) in the percentage of T<sub>FH</sub> cells in *Roquin<sup>san/san</sup> Sap<sup>-/-</sup>* mice relative to *Roquin<sup>san/san</sup>* mice ( $P = 0.0056$ ; Fig. 3 a, middle). SAP deficiency also resulted in a 10-fold reduction in the percentage of GC B cells in *Roquin<sup>san/san</sup>* mice ( $4.27 \pm 1.93\%$  vs.  $0.43 \pm 0.23\%$ ;  $P = 0.0007$ ; Fig. 3 b, middle). Immunohistochemistry paralleled the flow cytometry data, showing reduced size and number of GCs, and a reduction of T cell numbers within PNA-positive follicles (Fig. 3 c). These findings indicate that loss of SAP corrects the aberrant formation of T<sub>FH</sub> cells and the

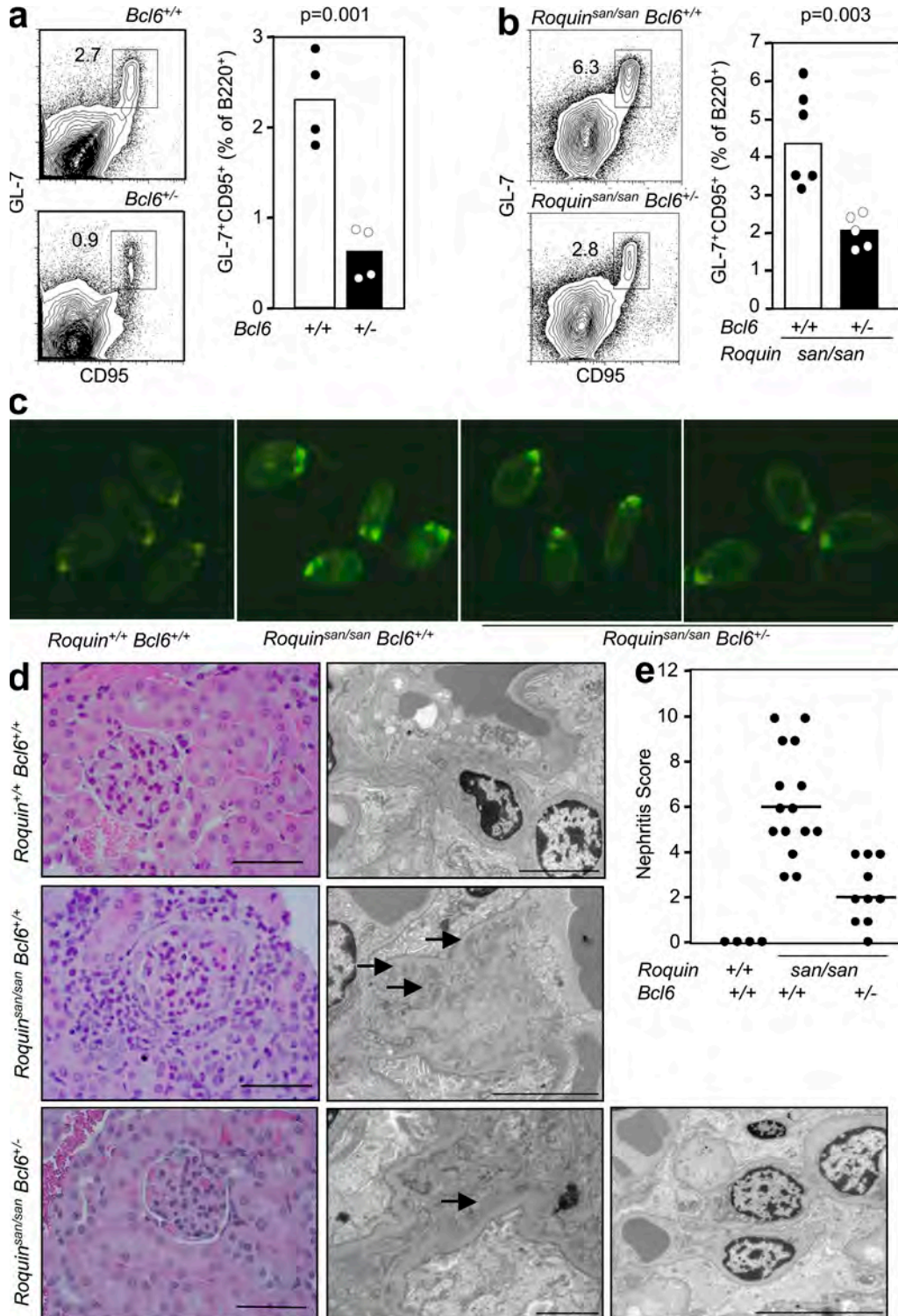


**Figure 1. Heterozygosity for Bcl6 reduces the magnitude of the GC response in *Roquin*<sup>+/+</sup> and *Roquin*<sup>san/san</sup> mice and ameliorates the lupus-like phenotype of *Roquin*<sup>san/san</sup> mice.** (a) Flow cytometric contour plots (left) and graphical analysis (right) of B220<sup>+</sup>GL-7<sup>+</sup>CD95<sup>+</sup> GC B cells in 10-wk-old wild-type (*Bcl6*<sup>+/+</sup>) and *Bcl6*<sup>+/-</sup> mice 8 d after SRBC immunization (P = 0.0011). Data are representative of four independent experiments (n = 4 per group). (b) Flow cytometric contour plots (left) and dot plots (right) showing B220<sup>+</sup>GL-7<sup>+</sup>CD95<sup>+</sup> GC B cells from 10-wk-old naive *Roquin*<sup>san/san</sup> *Bcl6*<sup>+/+</sup> and *Roquin*<sup>san/san</sup> *Bcl6*<sup>+/-</sup> mice. Data are representative of five independent experiments (n ≥ 4 per group). (c) Representative determination of serum IgG anti-dsDNA from 6-mo-old female *Roquin*<sup>+/+</sup> *Bcl6*<sup>+/+</sup>, *Roquin*<sup>san/san</sup> *Bcl6*<sup>+/+</sup>, and *Roquin*<sup>san/san</sup> *Bcl6*<sup>+/-</sup> mice, determined by immunofluorescence staining of *C. luciliae* substrate. Data shown reflect the occurrence (n ≥ 6 mice per group); three out of six *Roquin*<sup>san/san</sup> *Bcl6*<sup>+/-</sup> mice had low intensity staining (illustrated in the fourth panel from left),

inappropriate GC reaction phenotype of *Roquin<sup>san/san</sup>* to levels comparable to *Roquin<sup>+/+</sup>* mice.

To test whether loss of SAP alters other T effector subsets in *sanroque* mice, we quantified Th1 and Th2 cells by flow cytometric staining for Tbet and Gata3, respectively. There were no statistically significant differences in the percentage of CD44<sup>high</sup>GATA3<sup>+</sup>CD4<sup>+</sup> cells ( $0.91 \pm 0.14\%$  vs.  $1.15 \pm 0.41\%$ ;  $P = 0.18$ ) or CD44<sup>high</sup>Tbet<sup>+</sup>CD4<sup>+</sup> cells ( $6.76 \pm 10.6\%$  vs.  $8.66 \pm 5.74\%$ ;  $P = 0.59$ ) between *Roquin<sup>san/san</sup> Sap<sup>+/+</sup>* and *Roquin<sup>san/san</sup> Sap<sup>-/-</sup>* mice in peripheral blood (Fig. 4, a and b). Lymph node CD44<sup>high</sup>GATA3<sup>+</sup>CD4<sup>+</sup> cells ( $2.11 \pm 1.68\%$  vs.  $1.59 \pm 0.81\%$ ;  $P = 0.54$ ) and CD44<sup>high</sup>Tbet<sup>+</sup>CD4<sup>+</sup> cells ( $2.89 \pm 1.9\%$  vs.  $2.02 \pm 0.64\%$ ;  $P = 0.25$ ) between *Roquin<sup>san/san</sup> Sap<sup>+/+</sup>* and *Roquin<sup>san/san</sup> Sap<sup>-/-</sup>* mice were slightly reduced, but these differences were not statistically significant (Fig. 4 c). In contrast, SAP deficiency caused an approximately fourfold reduction in *Roquin<sup>san/san</sup>* lymph node T<sub>FH</sub> cells ( $3.93 \pm 0.47\%$  vs.  $1.11 \pm 0.38\%$ ;  $P = 0.001$ ; Fig. 4 c). Collectively, these data indicate that T<sub>FH</sub> cells are the T helper subset whose generation is most severely impaired by SAP deficiency in *Roquin<sup>san/san</sup>* mice.

#### Transfer of *Roquin<sup>san/san</sup>* T<sub>FH</sub> cells induces spontaneous GC reactions in wild-type mice

To test whether *Roquin<sup>san/san</sup>* T<sub>FH</sub> cells are sufficient to induce GC reactions in unimmunized wild-type mice, CD45.2<sup>+</sup> PD-1<sup>high</sup> CXCR5<sup>+</sup> CD44<sup>high</sup> CD4<sup>+</sup> T<sub>FH</sub> cells or CD45.2<sup>+</sup> PD-1<sup>-</sup> CXCR5<sup>-</sup> CD44<sup>high</sup> CD4<sup>+</sup> non-T<sub>FH</sub> T effector cells were adoptively transferred into CD45.1<sup>+</sup> C57BL/6 mice. 3 wk after transfer, 8% of donor T<sub>FH</sub> cells retained their CXCR5<sup>high</sup> PD-1<sup>high</sup> phenotype. In mice receiving non-T<sub>FH</sub> *san/san* CD-44<sup>high</sup> effectors, ~3% of the transferred cells had also acquired a comparable T<sub>FH</sub> phenotype (Fig. 4 d). Adoptive transfer of *Roquin<sup>san/san</sup>* T<sub>FH</sub> cells resulted in a threefold increase in the number of GC B cells compared with control mice injected with PBS alone ( $P = 0.003$ ; Fig. 4, e and f). A small increase in the percentage of GC cells was also observed in the mice that received non-T<sub>FH</sub> effector cells, although this was not statistically significant (Fig. 4, e and f). These data suggest that *Roquin<sup>san/san</sup>* T<sub>FH</sub> cells can drive a GC reaction in the absence of exogenous antigen.

#### SAP deficiency abrogates the lupus-like phenotype of *Roquin<sup>san/san</sup>* mice

Having established that SAP deficiency prevents T<sub>FH</sub> cell accumulation and selectively impairs GC responses, we sought to determine whether SAP deficiency affects the serum autoanti-

bodies and renal pathology of *Roquin<sup>san/san</sup>* mice. *Roquin<sup>san/san</sup> Sap<sup>-/-</sup>* mice had not developed ANAs by 8 wk of age (Fig. 5 a). Assessment of high-affinity anti-dsDNA IgG antibodies at 6 mo of age (by immunofluorescence using *Crithidia luciliae* substrate) revealed positive dsDNA antibodies in all *Roquin<sup>san/san</sup>* mice evaluated, whereas only one out of six *Roquin<sup>san/san</sup> Sap<sup>-/-</sup>* mice had detectable antibodies. Renal histology revealed that *Roquin<sup>san/san</sup> Sap<sup>-/-</sup>* mice had only minor interstitial nephritis and thickening of the mesangial matrix, with no detection of immune complex deposition observed by electron microscopy (Fig. 5, b and c). These data suggest that abrogation of signaling through SAP greatly reduced the autoimmune manifestations of *Roquin<sup>san/san</sup>* mice. In contrast, SAP deficiency conferred no significant reduction of splenomegaly, lymphadenopathy, and hypergammaglobulinemia present in *Roquin<sup>san/san</sup>* mice, indicating that these defects are not mediated by excessive T<sub>FH</sub> cell formation and GC function (Fig. S3, a–c, available at <http://www.jem.org/cgi/content/full/jem.20081886/DC1>).

#### Reduction of the GC response in *Roquin<sup>san/san</sup> Sap<sup>-/-</sup>* mice is mainly caused by B cell–extrinsic factors

Several studies have shown that SAP acts T cell intrinsically to regulate GC responses (35, 37, 39), but some controversy still exists in the light of one study showing B cell–intrinsic SAP-mediated effects (40). To test whether the correction of the GC response observed in *Roquin<sup>san/san</sup> Sap<sup>-/-</sup>* mice was caused by B cell–extrinsic factors, we transferred SW<sub>HEL</sub> B cells expressing intact SAP into *Roquin<sup>+/+</sup>*, *Roquin<sup>san/san</sup>*, *Sap<sup>-/-</sup>*, and *Roquin<sup>san/san</sup> Sap<sup>-/-</sup>* mice, in conjunction with hen egg lysozyme (HEL)<sup>2x</sup>–conjugated SRBCs.

Adoptively transferred SW<sub>HEL</sub> B cells formed HEL-specific GCs in all four cohorts. Significantly fewer GCs were observed in *Sap<sup>-/-</sup>* than in wild-type mice ( $23,958 \pm 15,920$  vs.  $1,186 \pm 1,019$ ;  $P = 0.005$ ; Fig. 5 d), confirming a B cell–extrinsic contribution of SAP to the GC response (34, 36, 38). In addition, SAP deficiency corrected the extreme GC formation observed in *Roquin<sup>san/san</sup>* mice ( $124,528 \pm 25,980$  vs.  $30,528 \pm 18,100$ ;  $P = 0.0004$ ) to a response of similar magnitude to *Roquin<sup>+/+</sup>* mice (Fig. 5 a). This suggests that the SAP-mediated effect in *Roquin<sup>san/san</sup>* mice is also caused by B cell–extrinsic factors, and is most likely caused by SAP's regulation of T<sub>FH</sub> cells.

To determine whether the loss of *Sap* in *Roquin<sup>san/san</sup>* mice selectively affected the GC response or also impaired the extrafollicular response, we identified donor-derived extrafollicular plasma cells containing intracellular anti-HEL Ig at day 5 after immunization (Fig. 5 e). At this time point, GC-derived

and three out of six were negative (illustrated in the third panel from left). (d) Representative images of kidney sections stained with H&E (left) or viewed under an electron microscope (right) from 6-mo-old mice of the indicated genotypes. *Roquin<sup>san/san</sup>* animals show widespread mesangial proliferative lesions with moderate interstitial infiltrate. There are multiple electron-dense deposits (arrows). Histological changes in *Roquin<sup>san/san</sup> Bcl6<sup>+/-</sup>* mice were mild, with occasional electron-dense deposits visible on electron microscopy in two individuals (far right). Images are representative ( $n \geq 4$  per group). Bars: (H&E) 100  $\mu$ m in all panels; (electron microscopy) 5  $\mu$ m in the *Roquin<sup>+/+</sup> Bcl6<sup>+/-</sup>* and *Roquin<sup>san/san</sup> Bcl6<sup>+/-</sup>* panels, 2  $\mu$ m in the left *Roquin<sup>san/san</sup> Bcl6<sup>+/-</sup>* panels, and 10  $\mu$ m in the right *Roquin<sup>san/san</sup> Bcl6<sup>+/-</sup>* panel. (e) Nephritis severity score of 6-mo-old female *Roquin<sup>+/+</sup>*, *Roquin<sup>san/san</sup>*, and *Roquin<sup>san/san</sup> Bcl6<sup>+/-</sup>* mice as determined by histological analysis according to the criteria given in Table S1 (available at <http://www.jem.org/cgi/content/full/jem.20081886/DC1>). Horizontal bars indicate medians. In a, b, and e, each symbol represents one mouse; p-values are indicated on the graphs, and the numbers in the plots represent percentages.

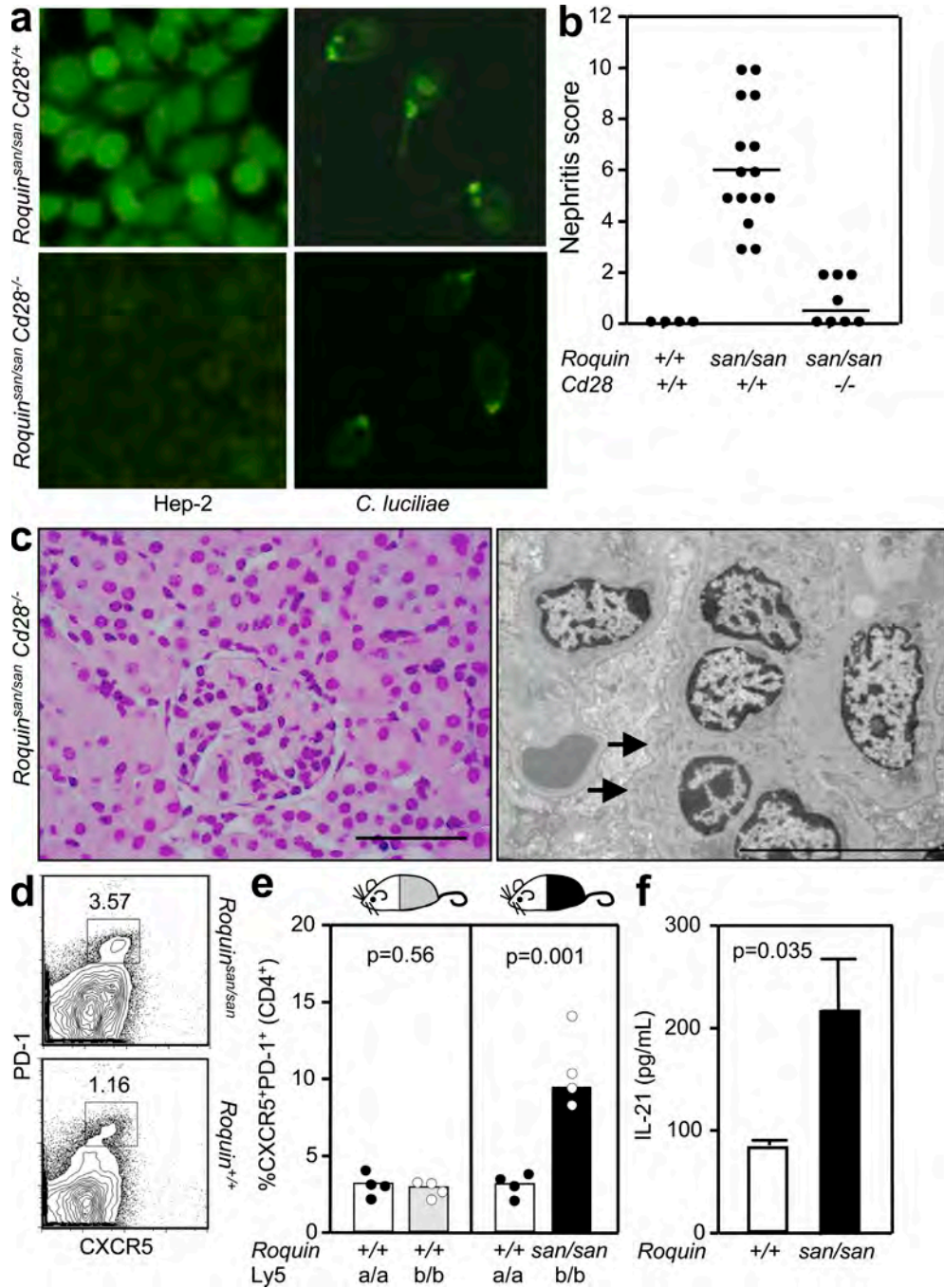


**Figure 2. The autoimmune phenotype of *Roquin<sup>san/san</sup>* mice requires T cell activation through CD28, and T<sub>FH</sub> cells are expanded cell autonomously.** (a, left) Detection of IgG-ANA using Hep-2 slides in sera from 8-wk-old female *Roquin<sup>san/san</sup>* and *Roquin<sup>san/san</sup> Cd28<sup>-/-</sup>* mice (*n* = 5 per group). (right) Detection of anti-dsDNA IgG serum antibodies in 6-mo-old female *Roquin<sup>san/san</sup>* and *Roquin<sup>san/san</sup> Cd28<sup>-/-</sup>* mice determined by staining *C. luciliae* slides. Data are representative of three independent experiments (*n* ≥ 5 per group). (b) Score of nephritis severity in 6-mo-old female *Roquin<sup>san/san</sup>* and *Roquin<sup>san/san</sup> Cd28<sup>-/-</sup>* mice as determined by histological analysis defined by the criteria given in Table S1 (available at <http://www.jem.org/cgi/content/full/jem.20081886/DC1>). Each symbol represents one mouse. Horizontal bars indicate medians. (c) Representative images of kidney sections stained with H&E (left) or viewed under an electron microscope (right). Histology from *Roquin<sup>san/san</sup> Cd28<sup>-/-</sup>* animals was much less severe, with normal H&E appearances and few electron-dense deposits (arrows) in the mesangium. Bars: (left) 100 μm; (right) 10 μm. (d) Representative flow cytometric contour plots of CD4<sup>+</sup>CXCR5<sup>+</sup>PD-1<sup>high</sup> T<sub>FH</sub> cells in 10-wk-old *Roquin<sup>san/san</sup>* mice and control littermates. Data are representative of five independent experiments (*n* = 4 per group), and the numbers in the plots represent percentages. (e) Dot plots representing percentages of CD4<sup>+</sup>CXCR5<sup>+</sup>PD-1<sup>high</sup> T<sub>FH</sub> cells from SRBC-immunized chimeric mice generated by reconstituting sublethally irradiated mice with a 1:1 mix of either *Roquin<sup>+/+</sup>.Ly5<sup>a</sup>*/*Roquin<sup>+/+</sup>.Ly5<sup>b</sup>* (left) or *Roquin<sup>+/+</sup>.Ly5<sup>a</sup>*/*Roquin<sup>san/san</sup>.Ly5<sup>b</sup>* (right). Data are representative of three independent experiments (*n* = 4 per group). Each symbol represents the Ly5<sup>a</sup> or

plasma cells cannot be detected (41). Although we observed a 4-fold decrease in SW<sub>HEL</sub> GC B cells, there was only a 1.3-fold decrease in the number of SW<sub>HEL</sub> extrafollicular plasma cells ( $53,198 \pm 1,528$  vs.  $40,528 \pm 7,548$ ;  $P = 0.04$ ) in *Roquin<sup>san/san</sup> Sap<sup>-/-</sup>* recipients compared with *Roquin<sup>san/san</sup> Sap<sup>+/+</sup>* controls (Fig. 5 e). These data suggest that the reduction of the GCs in *Roquin<sup>san/san</sup>* mice caused by *Sap* deficiency is mainly a result of B cell-extrinsic factors, and that this results in selective inhibition of the GC pathway.

### ***Roquin<sup>san/san</sup> Sap<sup>-/-</sup>* mice have reduced expression of ICOS and IL-21**

We have demonstrated that *Roquin<sup>san/san</sup> Sap<sup>-/-</sup>* mice have fewer T<sub>FH</sub> cells, a correction of the spontaneous GC response, and a reduction in autoimmune pathology. To gain insight into the possible functional T<sub>FH</sub> defect brought about by SAP deficiency in *Roquin<sup>san/san</sup>* mice, we quantified the changes in the expression of ICOS and IL-21, both of which are increased in *Roquin<sup>san/san</sup> CD4<sup>+</sup>* cells (22) and are shown to be essential for T<sub>FH</sub> cell formation, homeostasis, and function (33, 34, 42, 43). Loss of SAP reduced the levels of ICOS on both naive (CD44<sup>low</sup>) and activated/memory (CD44<sup>high</sup>) CD4<sup>+</sup> T cells in *Roquin<sup>san/san</sup>* mice and to an even greater extent on *Roquin<sup>+/+</sup>* mice (Fig. 6, a–c). Despite this reduction, *Roquin<sup>san/san</sup> Sap<sup>-/-</sup>* mice still expressed more than threefold higher levels of ICOS than *Roquin<sup>+/+</sup> Sap<sup>+/+</sup>* mice.

To determine whether loss of SAP had an effect on the production of IL-21, which was increased in *Roquin<sup>san/san</sup>* mice, we compared IL-21 production from *Roquin<sup>+/+</sup> Sap<sup>+/+</sup>*, *Roquin<sup>+/+</sup> Sap<sup>-/-</sup>*, *Roquin<sup>san/san</sup> Sap<sup>+/+</sup>*, and *Roquin<sup>san/san</sup> Sap<sup>-/-</sup>* splenocytes. SAP deficiency reduced IL-21 production by both *Roquin<sup>san/san</sup>* and *Roquin<sup>+/+</sup>* splenocytes (Fig. 6 d). Remarkably, the levels of IL-21 found in *Roquin<sup>san/san</sup> Sap<sup>-/-</sup>* cultures were comparable to those of wild-type (*Roquin<sup>+/+</sup> Sap<sup>+/+</sup>*) mice. As previously reported (37), SAP deficiency resulted in higher CD40L expression upon activation in both *Roquin<sup>+/+</sup>* and *Roquin<sup>san/san</sup>* mice (Fig. 6, e and f).

### **IL-21 deficiency does not prevent autoimmunity in *Roquin<sup>san/san</sup>* mice**

Given that *Roquin<sup>san/san</sup>* mice produce high levels of IL-21 and given the recently described role for IL-21 in T<sub>FH</sub> cell generation after immunization (33, 34), we investigated whether IL-21 also controls autoantibody production, T<sub>FH</sub> cell accumulation, and spontaneous GC formation in these mice. To this end, we crossed *Roquin<sup>san/san</sup>* mice to *IL-21<sup>-/-</sup>* mice on a C57BL/6 background and assessed ANA formation. There was no difference in the pattern or titer of ANAs produced by 10-wk-old *Roquin<sup>san/san</sup> IL-21<sup>+/+</sup>* and *Roquin<sup>san/san</sup> IL-21<sup>-/-</sup>* mice (Fig. 7, a and b). Overall, IL-21 deficiency did not affect the hypergammaglobulinemia of *Roquin<sup>san/san</sup>* mice (Fig. 7 c),

and consistent with previous reports (44), IgG1 titers were reduced, whereas IgE titers were increased (Fig. 7 c). Likewise, loss of IL-21 did not correct the lymphadenopathy or the splenomegaly of *Roquin<sup>san/san</sup>* mice (Fig. 7 d).

We then investigated whether IL-21 influences T<sub>FH</sub> cell accumulation and spontaneous GC formation. There was no difference in either the number of T<sub>FH</sub> cells or GC cells between *Roquin<sup>san/san</sup> IL-21<sup>+/+</sup>* and *Roquin<sup>san/san</sup> IL-21<sup>-/-</sup>* littermates, (Fig. 7, e and f). These data suggest that IL-21 does not play a role in spontaneous GC formation, T<sub>FH</sub> development, or accumulation in *Roquin<sup>san/san</sup>* mice.

## **DISCUSSION**

Elucidation of the defect that results in high-affinity antibodies to dsDNA is central to understanding lupus and, hence, the development of specific therapeutic interventions. In the *Roquin<sup>san/san</sup>* model, a fundamental GC defect results in the production of autoantibodies. This pathway appears to be critical for disease development, because an impediment to GC formation conferred by halving the dose of *Bcl6* is sufficient to attenuate the lupus phenotype. Our data are consistent with other evidence that aberrant T cell help can cause spontaneous GC formation and autoimmunity (9, 45). We show the expanded T<sub>FH</sub> cell subset, a consistent component of the *Roquin<sup>san/san</sup>* phenotype, is responsible for excessive GC formation. In *Roquin<sup>san/san</sup>* mice, GCs form in the absence of foreign antigen and yield ANAs. SAP deficiency reduces the size and activity of the T<sub>FH</sub> subset and abrogates autoantibody production and renal disease. These findings provide the in vivo cellular mechanism to link the defect in microRNA (miRNA)-mediated repression of T<sub>FH</sub> molecules conferred by the *san* allele of *Roquin* with the lupus phenotype of *Roquin<sup>san/san</sup>* mice (22, 28). Moreover, they elucidate a mechanism of lupus that could be generalized to other defects of T<sub>FH</sub> homeostasis. Importantly, they provide evidence that defects in positive selection of GC B cells can cause autoimmunity.

In this paper, we demonstrate that *Roquin<sup>san/san</sup>* acts T cell intrinsically to drive an accumulation of T<sub>FH</sub> cells that support a spontaneous GC response. Overexpression of ICOS is a plausible mechanism, because ICOS is important for the generation and survival of T<sub>FH</sub> cells (34, 42, 43), and *Roquin* normally acts to repress *Icos* miRNA (28). Previously, we have shown that this accounts for the lymphoproliferation, splenomegaly, and lymphadenopathy of *Roquin<sup>san/san</sup>* mice (28). The data presented in this paper also show that CD28 signaling is a key contributor to the development of systemic autoimmunity in *Roquin<sup>san/san</sup>* mice. CD28 is not only expressed on CD4<sup>+</sup> cells, but it has also been found to be expressed by stromal cells (46) and plasma cells (47), and this expression can influence B cell development and antibody responses. Nevertheless, our previous data showing that the increased plasma cell and GC

Ly5<sup>b</sup> population derived from one mouse. (f) ELISA was used to determine culture supernatant IL-21 levels from 24-h splenocyte cultures from *Roquin<sup>san/san</sup>* mice and littermate controls in the presence of PMA and ionomycin. Error bars indicate means  $\pm$  SEM. Data are representative of three independent tests where each sample was run in triplicate.

numbers, and B cell activation in *sanroque* are predominantly B cell extrinsic (22), together with the potent effects of SAP deficiency in the *sanroque* autoimmune phenotype, suggest that CD28 deficiency in T cells rather than in B cells or stromal cells

is responsible for the observed effect. Thus, we infer that the *sanroque* lupus phenotype is T cell mediated. CD28 deficiency considerably decreased the abnormally high levels of ICOS normally found on *Roquin<sup>san/san</sup>* T cells. This is likely to contribute

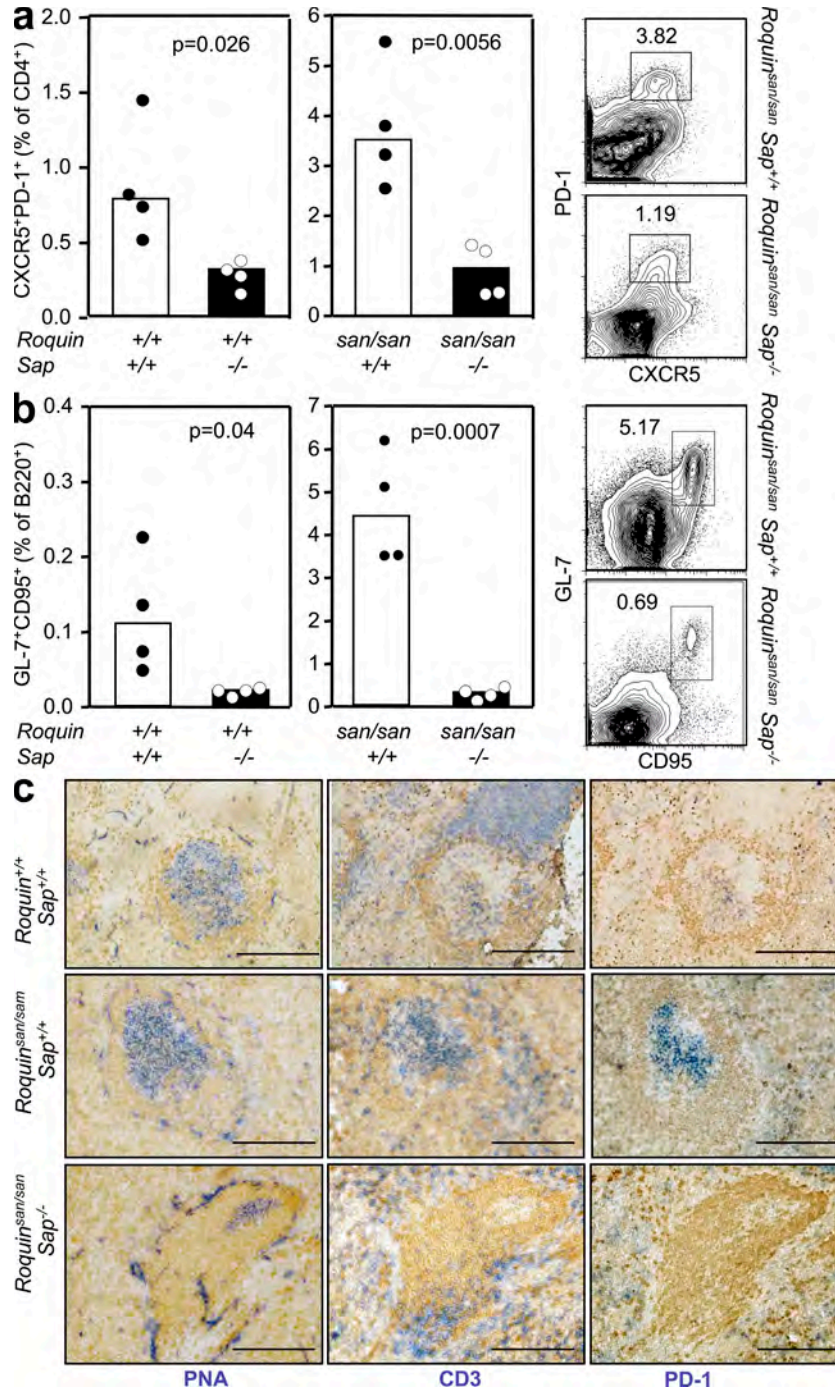


**Figure 3. Spontaneous GC and T<sub>FH</sub> formation are corrected by loss of SAP in *Roquin<sup>san/san</sup>* mice.** (a) CD4<sup>+</sup>CXCR5<sup>+</sup>PD-1<sup>high</sup> T<sub>FH</sub> cells in unimmunized 10-wk-old *Roquin<sup>san/san</sup>* and *Roquin<sup>san/san</sup> Sap<sup>-/-</sup>* mice (P = 0.0056). Representative flow cytometric contour plots are shown (right). Data are representative of four independent experiments (n = 4 per group). (b) B220<sup>+</sup>GL-7<sup>+</sup>CD95<sup>+</sup> GC B cells in unimmunized 10-wk-old *Roquin<sup>san/san</sup> Sap<sup>+/+</sup>* and *Roquin<sup>san/san</sup> Sap<sup>-/-</sup>* mice (P = 0.0007). Representative flow cytometric contour plots are shown (right). Data are representative of four independent experiments (n = 4 per group). (c) Photomicrographs of frozen spleen sections from unimmunized 6-mo-old mice of the indicated genotypes stained with IgD (brown; all panels), PNA (blue; left), TCRβ (blue; middle), and PD-1 (blue; right). Bars, 200 μm.

to the abrogation of the lupus phenotype in a manner comparable to halving the gene dose of *Icos* (28). A nonmutually exclusive explanation is that although ICOS overexpression

causes a lymphoproliferative syndrome, danger signals may also be required for the production of autoantibodies that cause end-organ damage. This is because ligands for CD28 are dependent

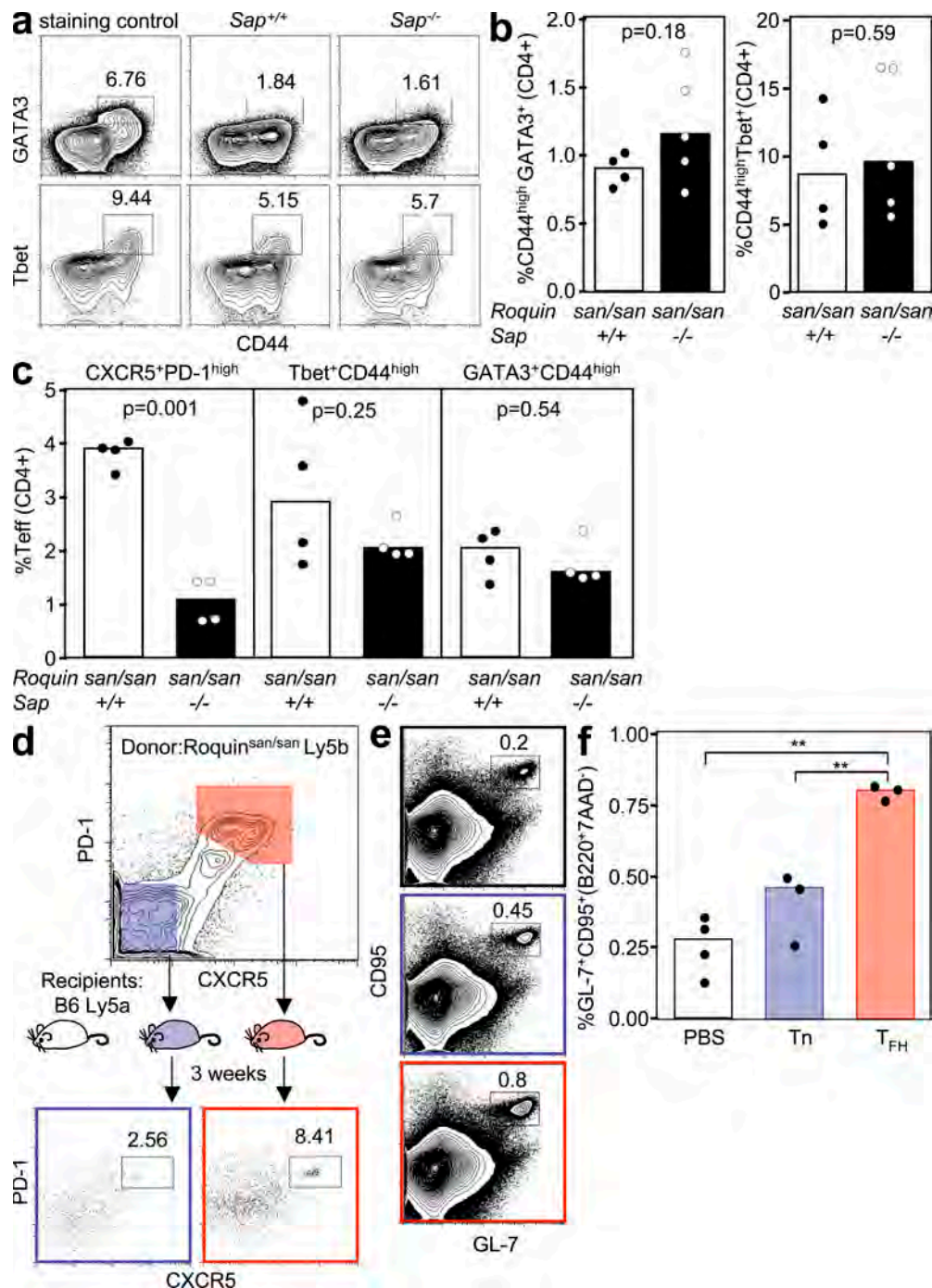


**Figure 4.** Th1 and Th2 cells are present in *Roquin*<sup>*san/san*</sup> mice in the absence of SAP and T<sub>FH</sub> cells, but not non-T<sub>FH</sub> effector cells, induce a GC response in wild-type mice. (a) Representative flow cytometric contour plots and (b) graphical analysis of GATA3<sup>+</sup>CD44<sup>high</sup>CD4<sup>+</sup> and Tbet<sup>+</sup>CD44<sup>high</sup>CD4<sup>+</sup> cells in mice of the indicated genotypes. Data are representative of two independent experiments ( $n \geq 4$  per group). (c) Representative dot plots of lymph node CD4<sup>+</sup>PD-1<sup>high</sup>CXCR5<sup>+</sup> (left), Tbet<sup>+</sup>CD44<sup>high</sup>CD4<sup>+</sup> (middle), and GATA3<sup>+</sup>CD44<sup>high</sup>CD4<sup>+</sup> (right) cells. (d) Experimental outline for adoptive transfer of *Roquin*<sup>*san/san*</sup> CD4<sup>+</sup> CD45.2 CD44<sup>high</sup> PD-1<sup>high</sup> CXCR5<sup>+</sup> or CD4<sup>+</sup> CD45.2 CD44<sup>high</sup> PD-1<sup>-</sup> CXCR5<sup>-</sup> T cells into CD45.1 C57BL/6 mice. (e) Flow cytometric contour plots and (f) dot plots of B220<sup>+</sup> GL-7<sup>+</sup> CD95<sup>+</sup> GC B cells from CD45.1 C57BL/6 recipients 3 wk after adoptive transfer of the indicated cell type. Data were generated from three mice per group (\*\*,  $P > 0.001$ ). In a, d, and e, the numbers in the plots represent percentages.

on Toll-like receptor ligation, which typically occurs during infections and tissue damage, and potentially after apoptosis. Because mice in this study were housed under specific pathogen-free conditions, one explanation for the source of the danger signal in the *san/san* model might be the abundance of apoptotic cells in GCs, which overloads the normal nonimmunogenic modes of disposal (11). Apoptotic cells display self-antigens that are the target of the autoimmune response in lupus, and are ligands for TLR7 and/or TLR9 on antigen-presenting cells and/or B cells (48).

Our data indicate that the GC is central to the autoimmune phenotype of *Roquin<sup>san/san</sup>* mice, because reduction of spontaneous GCs, conferred by halving the gene dose of the transcriptional regulator *Bcl6*, results in a proportionate amelioration of autoimmune pathology. This heterozygote phenotype is a novel finding. Although previous reports describe intact antibody responses in *Bcl6<sup>+/-</sup>* mice on day 11 after immunization (26), these are likely to derive predominantly from the extrafollicular response at this early time point. The heterozygote phenotype is consistent with the observation that GC differentiation is accompanied by only a twofold increase in *Bcl6* miRNA expression (49). Although our work does not exclude an effect of halving the gene dose of *Bcl6* on T<sub>FH</sub> cell formation, it does strongly suggest that the GC reduction seen in *Bcl6<sup>+/-</sup>* mice is a consequence of reduced B cell-expressed BCL6: in 50% *Bcl6<sup>+/+</sup>*/50% *Bcl6<sup>+/-</sup>* mixed bone marrow chimeras, GC B cells were only decreased in GC B cells deriving from *Bcl6<sup>+/-</sup>* bone marrow. Furthermore, transfer of *Bcl6<sup>+/+</sup>* SW<sub>HEL</sub> B cells into *Bcl6<sup>+/-</sup>* recipient mice, providing the major source of T<sub>FH</sub> cells, resulted in normal donor-derived GC numbers after HEL-SRBC immunization.

SAP deficiency abrogates autoimmunity in *Roquin<sup>san/san</sup>* mice. SAP deficiency affects several T cell subsets and natural killer cells (50, 51) but profoundly impairs the ability of T cells to provide help to B cells for GC formation (37–39). Our results demonstrate that SAP deficiency specifically reduces the development of CD4<sup>+</sup> T cells with a T<sub>FH</sub> phenotype, leaving Th1 and Th2 cell formation largely intact. This, together with the evidence presented for the GC dependence of autoimmunity, as well as the observation that transfer of *Roquin<sup>san/san</sup>* T<sub>FH</sub> cells induces spontaneous GC, places aberrant expansion of T<sub>FH</sub> cells at the root of spontaneous GC formation and autoimmunity in *Roquin<sup>san/san</sup>* mice. This mechanism is consistent with another lupus model, B6.Sle1<sup>Y<sup>aa</sup></sup>, in which T cells have a transcriptional profile typical of T<sub>FH</sub> cells (21).

SAP deficiency has been shown to ameliorate autoimmunity in another lupus-prone strain, MRL<sup>lpr</sup> mice (52). These mice have been shown to also develop spontaneous GCs (9), although SHM of autoreactive B blasts has been shown to occur in the T zone areas rather than within GCs (16). SAP deficiency has been shown to eliminate the pathogenic CD4<sup>-</sup>CD8<sup>-</sup> T cells that account for the lymphadenopathy of MRL<sup>lpr</sup> mice (52), and there is evidence that autoimmunity in MRL<sup>lpr</sup> mice is T cell dependent (53). It will be interesting to examine whether dysregulated ectopically located T<sub>FH</sub> cells or an extrafollicular counterpart is contributing to auto-

immunity in these mice. Finally, although *sanroque* SAP-deficient mice do not form spontaneous GCs, they still show hypergammaglobulinemia and very mild cell infiltrates in the kidney, suggesting that a non-T<sub>FH</sub>-mediated pathway contributes to these manifestations in *Roquin<sup>san/san</sup>* mice.

Our data add to previous studies demonstrating that SAP deficiency acts B cell extrinsically, causing a profound and selective impairment of GC reactions (37) with little effect on extrafollicular plasma cell generation. The requirement for SAP for effective T<sub>FH</sub> cell function has previously been ascribed to dysregulated kinetics of ICOS up-regulation and increased expression of CD40L (37), which we confirmed in the present study. Our work also shows that SAP signaling is required to maintain elevated baseline levels of ICOS in naive *sanroque* T cells.

An intriguing finding of this study was the lack of any role for IL-21 in *Roquin<sup>san</sup>*-induced lupus, T<sub>FH</sub> cell accumulation, and spontaneous GC formation. Although recent reports have shown that IL-21 is involved in T<sub>FH</sub> cell generation and optimal GC responses (33, 34), other groups have previously reported normal GC formation with an accumulation in IgG memory B cells in IL-21R<sup>-/-</sup> mice (54). A recent paper has also shown that IL-21 can be produced by extrafollicular T cells, which contribute to autoimmunity in MRL<sup>lpr</sup> mice (55). Furthermore, IL-21 has been shown to potently induce plasma cell generation from naive B cells (56), suggesting an important role for IL-21 in extrafollicular B cell responses. Even if IL-21 turns out to be critical for GC B cell selection, it is possible that other molecules overexpressed by *sanroque* T<sub>FH</sub> cells, such as ICOS, substitute for the effects normally mediated by IL-21.

The pathway to systemic autoimmunity identified in this paper highlights the importance of negative selection of self-reactive lymphocytes in GCs. Autoreactive B cells are a normal component of the naive peripheral B cell repertoire. In lupus patients, these cells enter GCs, whereas in healthy individuals, they are excluded (57). Other evidence indicates that in lupus, GCs can generate B cells that have antinuclear specificities from nonautoreactive precursors (7). Furthermore, GCs are increased in lupus (58). Regardless of their ontogeny, autoreactive centrocytes would normally fail to receive selection signals by T<sub>FH</sub> cells and would undergo apoptosis (59). Our data suggest that this process is perturbed by the *san* allele of *Roquin*.

According to the prevailing model for T<sub>FH</sub> selection of centrocytes, large numbers of GC B cells compete with each other for the limiting available T cell help (60) and for antigen on follicular dendritic cells. Centrocytes that have acquired higher affinity for antigen would scavenge more antigen from follicular dendritic cells, which would confer on them an avidity advantage in interactions with T<sub>FH</sub> cells compared with lower affinity B cells. Based on this model, we speculate that in *Roquin<sup>san/san</sup>* mice, competition by B cells for T cell help is reduced by the expansion of T<sub>FH</sub> cells. Interactions between centrocytes and T<sub>FH</sub> cells are determined by affinity for MHC-peptide for the TCR modified by the action of accessory molecules. Loss of SAP in *Roquin<sup>san/san</sup>* mice causes a reduction in ICOS overexpression, potentially increasing the

antigen affinity required to reach the  $T_{FH}$  activation threshold in *Roquin<sup>san/san</sup> Sap<sup>-/-</sup>* mice.

Although the lupus phenotype of *Roquin<sup>san/san</sup>* mice is Mendelian, apart from rare exceptions (61), lupus is a polygenic disorder. Nevertheless, it is plausible that one or more polymorphisms or mutations that affect  $T_{FH}$  homeostasis, such as

those that regulate IL-21, ICOS, or ICOSL expression, could contribute to lupus pathogenesis. Because  $T_{FH}$  cells are present in peripheral blood, this is a testable hypothesis. Indeed, there is evidence that SLE patients have increased numbers of circulating  $CD4^+ICOS^+$  cells in their peripheral blood compared with nonautoimmune individuals (62). Because  $T_{FH}$  cells are

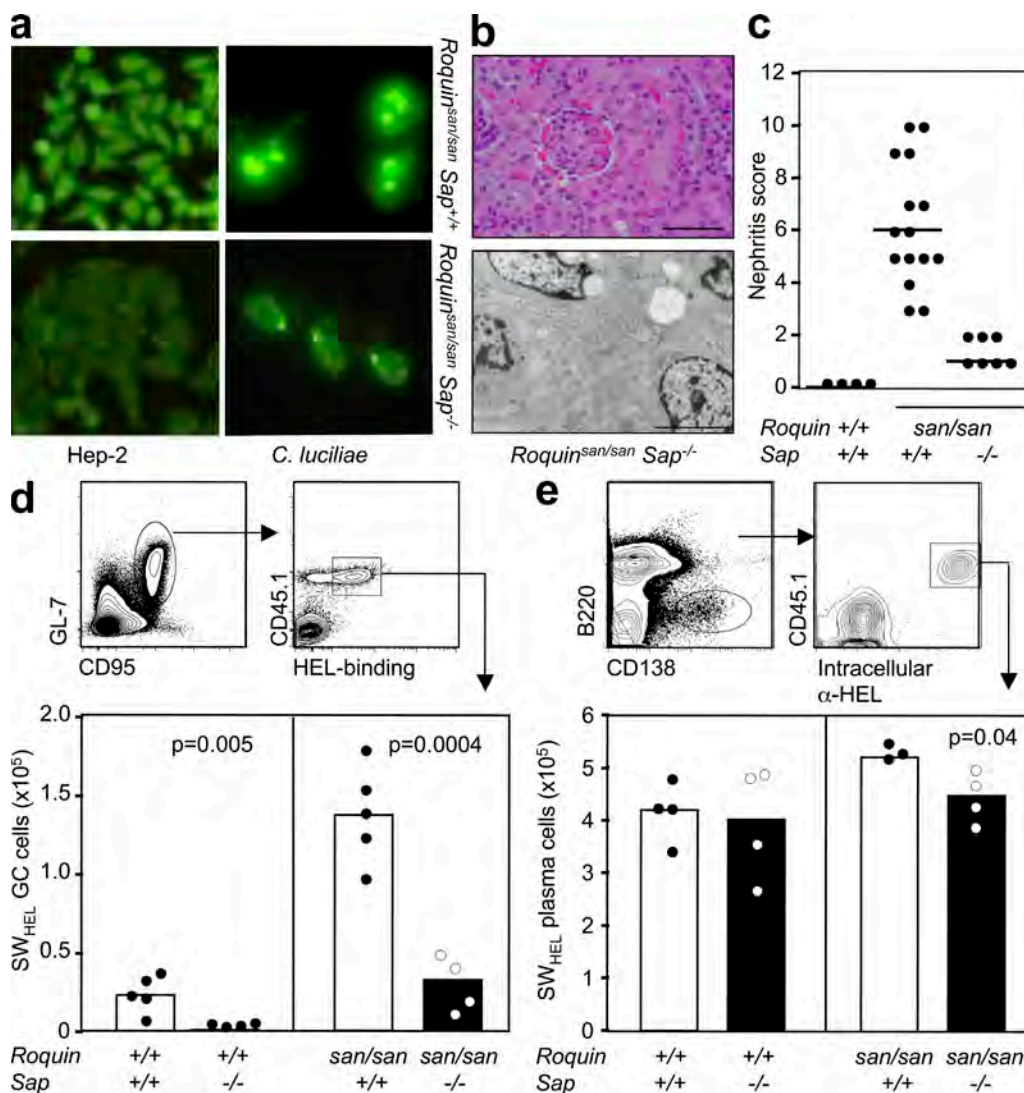


**Figure 5. Serum autoantibodies and renal pathology in *Roquin<sup>san/san</sup> Sap<sup>-/-</sup>* mice and reduction of the GC response in SAP-deficient *Roquin<sup>san/san</sup>* mice is caused by B cell-extrinsic factors.** (a, left) Representative staining of Hep-2 slides for detection of IgG ANA in the serum of 8-wk-old female *Roquin<sup>san/san</sup>* and *Roquin<sup>san/san</sup> Sap<sup>-/-</sup>* mice ( $n = 5$  per group). (right) Detection of IgG anti-dsDNA serum antibodies in 6-mo-old female *Roquin<sup>san/san</sup>* and *Roquin<sup>san/san</sup> Sap<sup>-/-</sup>* mice determined by immunofluorescence staining using *C. luciliae* substrate. Data are representative of three independent experiments ( $n \geq 5$  per group). (b) Representative images of kidney sections stained with H&E (top) or viewed under an electron microscope (bottom) from 6-mo-old female *Roquin<sup>san/san</sup> Sap<sup>-/-</sup>* mice. *Roquin<sup>san/san</sup> Sap<sup>-/-</sup>* mice show slight mesangial expansion on H&E staining but no electron-dense deposits. Bars: (top) 100  $\mu$ m; (bottom) 5  $\mu$ m. (c) Score of nephritis severity in 6-mo-old female *Roquin<sup>+/+</sup>*, *Roquin<sup>san/san</sup>*, and *Roquin<sup>san/san</sup> Sap<sup>-/-</sup>* mice as determined by histological analysis according to the criteria given in Table S1 (available at <http://www.jem.org/cgi/content/full/jem.20081886/DC1>). Each symbol represents one mouse. Horizontal bars indicate medians. (d) Gating strategy for assessing the HEL-specific GC response (top) and graphic representation (bottom) of the total number of HEL-specific GC cells per spleen in mice with the indicated genotypes 7 d after cotransfer of SW<sub>HEL</sub> B cells and HEL<sup>2x</sup>-conjugated SRBCs. Data are representative of three independent experiments ( $n \geq 4$ ). Each symbol represents one mouse. (e) Gating strategy for determining HEL-specific extrafollicular plasma cells (top) and graphical representation (bottom) of the number of HEL-specific plasma cells 5 d after cotransfer into mice with the indicated genotypes. Data are representative of two independent experiments ( $n \geq 3$  per group).  $p$ -values are indicated on graphs.

the cells expressing the highest levels of ICOS (63, 64), it is possible that circulating CD4<sup>+</sup>ICOS<sup>+</sup> cells reflect an excessive T<sub>FH</sub> response, and is consistent with recent data showing that a subset of SLE patients have an increased proportion of CD4<sup>+</sup>C D45RO<sup>+</sup>CXCR5<sup>+</sup>ICOS<sup>high</sup>PD-1<sup>high</sup> cells in their peripheral

blood (a phenotype that correlates with higher titers of anti-dsDNA antibodies and more severe kidney damage; unpublished data). If confirmed in independent studies, the GC-T<sub>FH</sub> pathway elucidated in the *Roquin<sup>san/san</sup>* model pathway would emerge as a novel and specific target for therapy.

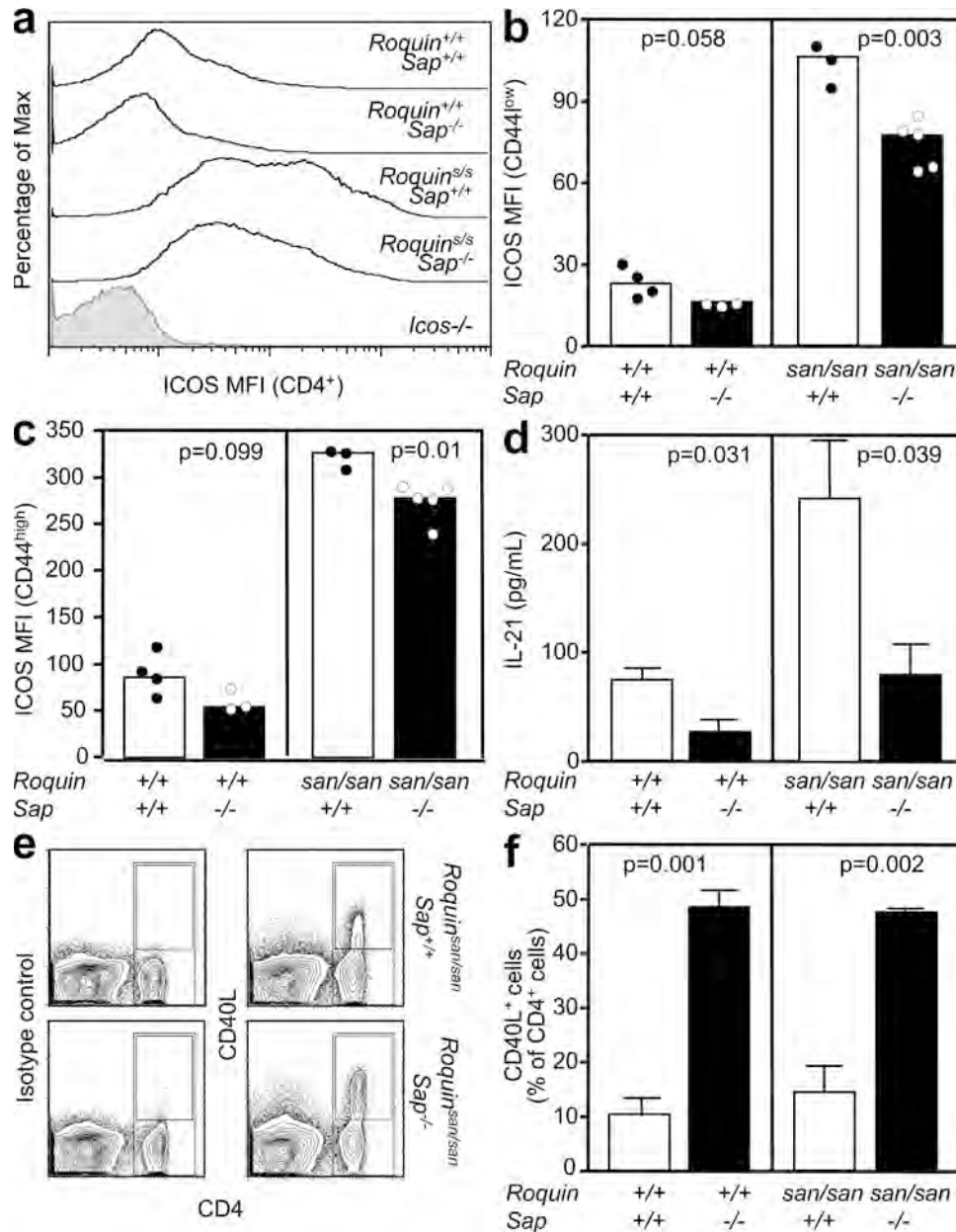


**Figure 6.** T<sub>FH</sub> cell-associated molecules are decreased in *Roquin<sup>san/san</sup> Sap<sup>-/-</sup>* mice. (a) Representative flow cytometric histograms and (b and c) graphical analysis showing ICOS mean fluorescence intensity (MFI) of splenic naive CD44<sup>low</sup> (b) and activated/memory CD44<sup>high</sup> (c) CD4<sup>+</sup> T cells from 10-wk-old unimmunized mice of the indicated genotypes. Data are representative of three independent experiments. Each symbol represents one mouse. (d) ELISA quantification of IL-21 in supernatant from an overnight culture of splenocytes in the presence of PMA and ionomycin from mice of the indicated genotypes. Data are representative of three experiments. (e) Flow cytometric contour plots of CD40L expression on splenocytes, 5 h after stimulation with anti-CD3 and anti-CD28, derived from mice of the indicated genotypes. (left) Staining with an isotype control; (right) CD40L staining. (f) Histograms of the percentage of CD4<sup>+</sup> cells that express CD40L (gated as shown in e) 5 h after CD3 and CD28 stimulation on splenocytes from mice with the indicated genotypes. In d and f, error bars indicate means ± SEM.

## MATERIALS AND METHODS

**Mice and immunizations.** *Roquin<sup>san/san</sup>* and C57BL/6 (B6) mice, all crossed to *Sap<sup>-/-</sup>*, *Bd6<sup>+/-</sup>*, *Cd28<sup>-/-</sup>*, and *IL-21<sup>-/-</sup>* mice, and SW<sub>HEL</sub> mice, were

housed in specific pathogen-free conditions at the Australian National University Bioscience Facility. IL-21 KO mice were generated at Lexicon Pharmaceuticals, Inc. and were provided by M. Smyth (Peter MacCallum Cancer

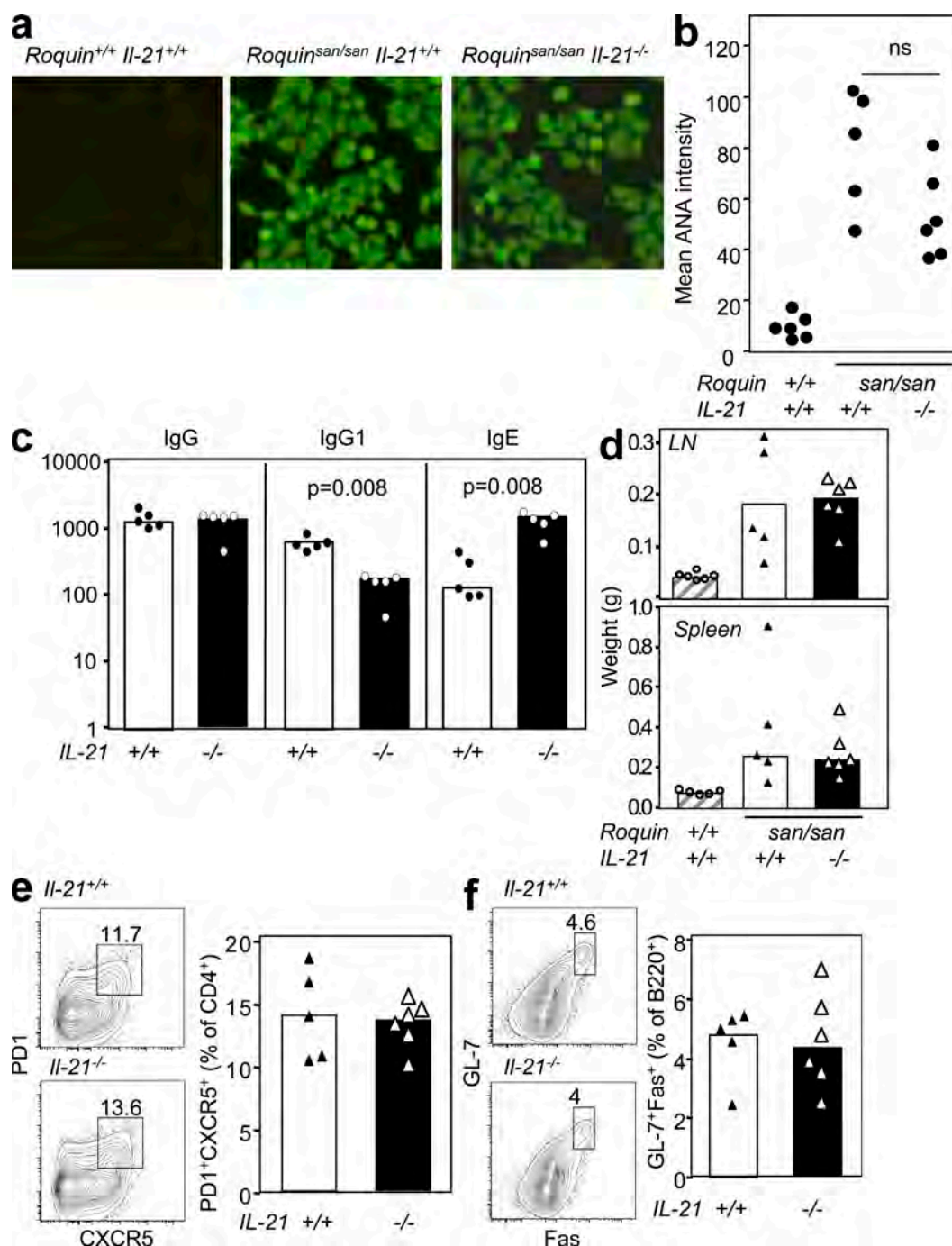


**Figure 7. Lack of IL-21 does not affect the phenotype,  $T_{FH}$  cell accumulation, or GC formation of *Roquin<sup>san/san</sup>* mice.** (a) IgG ANAs in the serum of mice of the genotypes indicated, detected by immunofluorescence using Hep-2 substrate. Data are representative of three independent experiments ( $n \geq 5$  mice per group). (b) Score of ANA staining intensity by confocal microscopy from sera taken from mice of the indicated genotypes. Data are representative of three independent experiments ( $n \geq 5$  mice per group). (c) Basal serum total IgG, IgG1, and IgE measured by ELISA. Data are representative of two independent experiments ( $n = 5$  mice per group). (d) Lymph node and spleen weight in grams for mice of the indicated genotypes. Data are representative of two independent experiments ( $n \geq 5$  per group). (e) Flow cytometric contour plots and dot plots of  $PD1^{high}CXCR5^{+}CD4^{+}$   $T_{FH}$  cells and (f)  $GL-7^{+}CD95^{+}B220^{+}$  GC cells from mice of the indicated genotypes. Data are representative of two independent experiments ( $n \geq 5$  mice per group). In e and f, the numbers in the plots represent percentages.

Centre, Melbourne, Australia) and ZymoGenetics, Inc. These mice were backcrossed 10 generations onto the C57BL/6 background. SW<sub>HEL</sub> mice carry a Vk10- $\kappa$  light chain transgene and a knocked in VH10 Ig heavy chain in place of the JH segments of the endogenous IgH gene that encode a high-affinity antibody for HEL (65). All animal procedures were approved by the Australian National University Animal Ethics and Experimentation Committee.

To generate thymus-dependent responses where indicated in the figures, 8–12-wk-old mice were immunized i.p. with  $2 \times 10^9$  SRBCs (Institute of Medical and Veterinary Science Veterinary Services). For experiments involving SW<sub>HEL</sub> mice,  $10^4$  SW<sub>HEL</sub> B cells were transferred into recipients, which were simultaneously immunized i.v. with  $2 \times 10^8$  SRBCs conjugated with mutant HEL<sup>2x</sup> using a protein conjugation kit (Invitrogen) (41).

**Bone marrow chimeras.** Recipient C57BL/6-Ly5a mice were sublethally irradiated with 1,000 Rad and were reconstituted via i.v. injection with  $2 \times 10^6$  donor bone marrow-derived hematopoietic stem cells.

**Antibodies.** Antibodies and streptavidin conjugates for flow cytometry were from BD unless otherwise indicated: anti-mouse B220-PerCP, CD4-PerCP, ICOS-PE (eBioscience), FoxP3 (eBioscience), GL-7-FITC, GATA3-allophycocyanin, Tbet-PerCP Cy5.5, CD95-PE, CXCR5-biotin, PD-1-PE (eBioscience), CTLA-4-PE, CD25-allophycocyanin, streptavidin-PerCP Cy5.5, and CD40L-biotin. For immunohistochemistry, the primary antibodies and reagents used were rat anti-mouse IgD (SouthernBiotech), biotinylated anti-mouse TCR $\beta$  (BD), rat anti-mouse PD-1 (BioLegend), and PNA-biotin (Vector Laboratories); the secondary antibody used was rabbit anti-rat horseradish peroxidase (HRP; Dako).

**Cell isolation, culture, and stimulation.** Single-cell suspensions were prepared from spleens of unimmunized and/or immunized mice. Single-cell suspensions were prepared in RPMI 1640 medium (JRH Biosciences) supplemented with 2 mM L-Glutamine (Invitrogen), 100 U penicillin-streptomycin (Invitrogen), 0.1 mM nonessential amino acids (Invitrogen), 100 mM Hepes (Sigma-Aldrich),  $5 \times 10^{-5}$  2-mercaptoethanol, and 10% fetal calf serum by sieving and gentle pipetting through 70- $\mu$ m nylon mesh filters (Falcon; BD). Cells were then cultured for 24 h at 37°C/5% CO<sub>2</sub> with 50 ng/ml PMA (Sigma-Aldrich) and 1  $\mu$ M ionomycin (Sigma-Aldrich) in triplicate wells. Cell culture supernatants were aspirated for further analysis by ELISA. For CD40L expression, cells were cultured in triplicate wells for 5 h in 96-well plates (Costar; Corning) with platebound 1  $\mu$ g/ml anti-CD3 (BD) and 10  $\mu$ g/ml anti-CD28 (BD). Biotinylated anti-CD40L antibody was added 2 h before harvesting.

**Flow cytometry.** For surface staining, single-cell suspensions were prepared as described in the previous section, and cells were maintained in the dark at 4°C throughout. Cells were washed twice in ice-cold FACS buffer (2% fetal calf serum, 0.1% NaN<sub>3</sub> in PBS), and incubated with each antibody and conjugate layer for 30 min and washed thoroughly with FACS buffer between each layer. Intracellular staining was performed using the Cytotfix/Cytoperm kit (BD) according to the manufacturer's instructions. For detection of HEL-binding B cells, HEL was conjugated to Alexa Fluor 647 using the manufacturer's instructions (Invitrogen). A FACSCalibur (BD) with CellQuest software (BD) was used for the acquisition of flow cytometric data, and FlowJo software (Tree Star, Inc.) was used for analysis.

**Adoptive cell transfer experiments.** T<sub>FH</sub> cells (CD4<sup>+</sup>CD44<sup>high</sup>PD-1<sup>high</sup>CXCR5<sup>high</sup>) and non-T<sub>FH</sub> effector cells (CD4<sup>+</sup>CD44<sup>high</sup>PD-1<sup>int/lo</sup>CXCR5<sup>-</sup>) from spleens and lymph nodes were prepared and stained as described in the previous paragraph and sorted on a FACSAria (BD).  $5 \times 10^6$  sorted cells were resuspended in PBS and injected into the tail vein of unmanipulated CD45.1 C57BL/6 recipients. 3-wk after transfer, splenic donor (CD45.2) T<sub>FH</sub> cells and host GC cells were enumerated by flow cytometry.

**ELISA.** Maxisorb plates (Thermo Fisher Scientific) were coated with 100  $\mu$ g/ml of recombinant mouse IL-21R/Fc (R&D Systems). Serial supernatant dilutions

were applied in quadruplicate, and IL-21 concentration was determined with 200 ng/ml of HRP-conjugated goat anti-mouse IL-21 IgG (R & D systems). Bound IL-21 was detected using phosphatase substrate tablets (Sigma-Aldrich). Plates were read at 405 nm using a microplate reader (Thermomax; MDS Analytical Technologies). The titers for supernatant samples were calculated according to the standard curve generated using twofold dilutions of recombinant mouse IL-21 (500–15 pg/ml; R&D Systems) and Prism software (GraphPad Software, Inc.). IL-17 ELISA was performed using the mouse IL-17A ELISA Ready-Set-Go! Kit (eBioscience) according to the manufacturer's instructions.

For analysis of total IgG, IgG1, and IgE titers, Maxisorb plates were coated with goat anti-mouse  $\kappa$  light chain or anti-mouse IgE (BD). Serial serum dilutions were applied, and Ig concentration was determined with HRP-conjugated goat anti-mouse IgG, IgG1 (SouthernBiotech), or biotinylated IgE (BD), followed by streptavidin-HRP. The enzyme bound to plates was developed using phosphatase substrate tablets. Plates were read at 405 nm using a Thermomax microplate reader. The titers for serum samples were calculated as the log serum concentration required to achieve 50% maximum OD.

**Immunohistochemistry.** 5- $\mu$ m acetone-fixed frozen sections of spleen were air dried and washed in 0.1 M Tris-buffered saline (TBS), pH 7.6, and were stained with various antibodies for 45 min at room temperature in a moist chamber. After a further wash in TBS, secondary reagents, previously absorbed in 10% normal mouse serum, were added to the sections for 45 min. Where biotin-conjugated primary or secondary reagents were used, streptavidin alkaline phosphatase (Vector Laboratories) was added after a further wash in TBS and incubated for 20 min. HRP activity was detected using diaminobenzidine tetrahydrochloride solution (Sigma-Aldrich) and hydrogen peroxide. Alkaline phosphatase activity was detected using the AP Substrate Kit III (Vector Laboratories). Sections were mounted with IMMU-MOUNT (Thermo Shandon) and viewed under a microscope (model IX71; Olympus).

**Renal pathology.** Kidneys were fixed in 10% neutral buffered formalin. 4- $\mu$ m paraffin-embedded sections were dewaxed and stained with hematoxylin and eosin (H&E) and silver stains. For electron microscopy, kidneys were fixed in 2% glutaraldehyde in 0.1 M cacodylate buffer, pH 7.4, at room temperature overnight. They were then washed in 0.1 M cacodylate buffer, treated with 0.2 mm of filtered 2% osmium tetroxide in 0.1 M cacodylate buffer, pH 7.4, at room temperature for 2 h, and washed in double-distilled H<sub>2</sub>O. Samples were stained with 0.2 mm of filtered 2% aqueous uranyl acetate for 30 min at room temperature, dehydrated in ethanol, and embedded in 100% TAAB medium mix, low viscosity resin. They were then mounted in orientation silicone molds and heated in an oven at 70°C for 8–12 h. The samples were examined on a transmission electron microscope (model 1011; JEOL) at 60 KeV. The images were captured using a digital camera (Mega-View III) and the AnalySIS software package (Soft Imaging System; Olympus), and were subsequently scored using the criteria detailed in Table S1 (available at <http://www.jem.org/cgi/content/full/jem.20081886/DC1>).

**ANA and dsDNA assessment.** Serum obtained by eye bleed from 8-wk-old mice was diluted in PBS 1:40 and used for indirect immunofluorescence on fixed Hep-2 slides (Antibodies, Inc.) for ANA detection, and serum from 6-mo-old mice was diluted 1:20 and used for indirect immunofluorescence on fixed *C. luciliae* slides (Antibodies, Inc.) for ANA anti-dsDNA antibody detection, respectively. Alexa Fluor 488 goat anti-mouse IgG (Invitrogen) was used to detect mouse antibodies. Autoantibodies were scored blind as negative or positive on a scale of 1–3 based on the intensity of fluorescence. Relative levels of ANAs were estimated by viewing the slides using a confocal microscope (TCS SP5; Leica) at 20 $\times$  magnification and a fixed laser power, and measuring the fluorescence of five randomly selected 1,250- $\mu$ m<sup>2</sup> regions of Hep2 cells, compared with five regions where cells were absent. The sample-specific mean background was subtracted from the sample-specific mean fluorescence to give an estimation of fluorescent intensity. These results concurred with a blinded manual scoring of fluorescence for the same samples.

**Statistical analysis.** Data were analyzed using a two-tailed Student's *t* test using Prism software.

**Online supplemental material.** Fig. S1 illustrates that the loss of one allele of Bcl6 results in B cell–intrinsic defects in GC formation. Fig. S2 a shows that CD4<sup>+</sup>FoxP3<sup>+</sup> T reg cells are expanded twofold in *Roquin<sup>san/san</sup>* mice relative to *Roquin<sup>+/+</sup>* mice. Fig. S2 b demonstrates that *Roquin<sup>san/san</sup>* splenocytes produce equivalent levels of IL-17 to *Roquin<sup>+/+</sup>* splenocytes. Fig. S3 (a and b) shows that *Sap* deficiency does not correct the splenomegaly and lymphadenopathy in *Roquin<sup>san/san</sup>* mice. Fig. S3 c demonstrates that hyper-IgG in *Roquin<sup>san/san</sup>* mice is not corrected in the absence of *Sap*. Table S1 describes the scoring strategy used to assess the severity of mouse nephritis. Online supplemental material is available at <http://www.jem.org/cgi/content/full/jem.20081886/DC1>.

We thank C. Goodnow for helpful discussions of this work, A. Prins for kidney sectioning, T. Chan for preparing HEL2<sup>x</sup>-conjugated SRBCs for SW<sub>HEL</sub> experiments, M. Townsend for cutting frozen spleen sections, and M. Smyth and ZymoGenetics, Inc. for providing us with the IL-21<sup>-/-</sup> mice.

This work was funded by a Viertel Senior Medical Research Fellowship and National Health and Medical Research Council grants 316956 and 427620 to C.G. Vinuesa.

The authors have no conflicting financial interests.

Submitted: 21 August 2008

Accepted: 22 January 2009

## REFERENCES

- Hochberg, M.C. 1997. Updating the American College of Rheumatology revised criteria for the classification of systemic lupus erythematosus. *Arthritis Rheum.* 40:1725.
- Arbuckle, M.R., M.T. McClain, M.V. Rubertone, R.H. Scofield, G.J. Dennis, J.A. James, and J.B. Harley. 2003. Development of autoantibodies before the clinical onset of systemic lupus erythematosus. *N. Engl. J. Med.* 349:1526–1533.
- Rahman, A., and D.A. Isenberg. 2008. Systemic lupus erythematosus. *N. Engl. J. Med.* 358:929–939.
- MacLennan, I.C., K.M. Toellner, A.F. Cunningham, K. Serre, D.M. Sze, E. Zuniga, M.C. Cook, and C.G. Vinuesa. 2003. Extrafollicular antibody responses. *Immunol. Rev.* 194:8–18.
- Jacob, J., G. Kelsoe, K. Rajewsky, and U. Weiss. 1991. Intraclonal generation of antibody mutants in germinal centers. *Nature.* 354:389–392.
- MacLennan, I.C. 1994. Germinal centers. *Annu. Rev. Immunol.* 12:117–139.
- Diamond, B., J.B. Katz, E. Paul, C. Aranow, D. Lustgarten, and M.D. Scharff. 1992. The role of somatic mutation in the pathogenic anti-DNA response. *Annu. Rev. Immunol.* 10:731–757.
- Behar, S.M., D.L. Lustgarten, S. Corbet, and M.D. Scharff. 1991. Characterization of somatically mutated S107 VH11-encoded anti-DNA autoantibodies derived from autoimmune (NZB × NZW)F1 mice. *J. Exp. Med.* 173:731–741.
- Luzina, I.G., S.P. Atamas, C.E. Storrer, L.C. daSilva, G. Kelsoe, J.C. Papadimitriou, and B.S. Handwerker. 2001. Spontaneous formation of germinal centers in autoimmune mice. *J. Leukoc. Biol.* 70:578–584.
- Casciola-Rosen, L.A., G. Anhalt, and A. Rosen. 1994. Autoantigens targeted in systemic lupus erythematosus are clustered in two populations of surface structures on apoptotic keratinocytes. *J. Exp. Med.* 179:1317–1330.
- Hanayama, R., M. Tanaka, K. Miyasaka, K. Aozasa, M. Koike, Y. Uchiyama, and S. Nagata. 2004. Autoimmune disease and impaired uptake of apoptotic cells in MFG-E8-deficient mice. *Science.* 304:1147–1150.
- Weller, S., M.C. Braun, B.K. Tan, A. Rosenwald, C. Cordier, M.E. Conley, A. Plebani, D.S. Kumararatne, D. Bonnet, O. Tournilhac, et al. 2004. Human blood IgM “memory” B cells are circulating splenic marginal zone B cells harboring a prediversified immunoglobulin repertoire. *Blood.* 104:3647–3654.
- Kim, J.H., J. Kim, Y.S. Jang, and G.H. Chung. 2006. Germinal center-independent affinity maturation in tumor necrosis factor receptor 1-deficient mice. *J. Biochem. Mol. Biol.* 39:586–594.
- Shlomchik, M.J., A.H. Aucocin, D.S. Pisetsky, and M.G. Weigert. 1987. Structure and function of anti-DNA autoantibodies derived from a single autoimmune mouse. *Proc. Natl. Acad. Sci. USA.* 84:9150–9154.
- Shlomchik, M.J., A. Marshak-Rothstein, C.B. Wolfowicz, T.L. Rothstein, and M.G. Weigert. 1987. The role of clonal selection and somatic mutation in autoimmunity. *Nature.* 328:805–811.
- William, J., C. Euler, S. Christensen, and M.J. Shlomchik. 2002. Evolution of autoantibody responses via somatic hypermutation outside of germinal centers. *Science.* 297:2066–2070.
- Groom, J.R., C.A. Fletcher, S.N. Walters, S.T. Grey, S.V. Watt, M.J. Sweet, M.J. Smyth, C.R. Mackay, and F. Mackay. 2007. BAFF and MyD88 signals promote a lupuslike disease independent of T cells. *J. Exp. Med.* 204:1959–1971.
- Yokoyama, T., M. Tanahashi, Y. Kobayashi, Y. Yamakawa, M. Maeda, T. Inaba, M. Kiriya, I. Fukai, and Y. Fujii. 2002. The expression of Bcl-2 family proteins (Bcl-2, Bcl-x, Bax, Bak and Bim) in human lymphocytes. *Immunol. Lett.* 81:107–113.
- Liu, Y.J., D.E. Joshua, G.T. Williams, C.A. Smith, J. Gordon, and I.C. MacLennan. 1989. Mechanism of antigen-driven selection in germinal centers. *Nature.* 342:929–931.
- Vinuesa, C.G., S.G. Tangye, B. Moser, and C.R. Mackay. 2005. Follicular B helper T cells in antibody responses and autoimmunity. *Nat. Rev. Immunol.* 5:853–865.
- Subramanian, S., K. Tus, Q.Z. Li, A. Wang, X.H. Tian, J. Zhou, C. Liang, G. Bartov, L.D. McDaniel, X.J. Zhou, et al. 2006. A Tlr7 translocation accelerates systemic autoimmunity in murine lupus. *Proc. Natl. Acad. Sci. USA.* 103:9970–9975.
- Vinuesa, C.G., M.C. Cook, C. Angelucci, V. Athanasopoulos, L. Rui, K.M. Hill, D. Yu, H. Domaschenz, B. Whittle, T. Lambe, et al. 2005. A RING-type ubiquitin ligase family member required to repress follicular helper T cells and autoimmunity. *Nature.* 435:452–458.
- Hsu, H.C., P. Yang, J. Wang, Q. Wu, R. Myers, J. Chen, J. Yi, T. Guentert, A. Tousson, A.L. Stanus, et al. 2008. Interleukin 17-producing T helper cells and interleukin 17 orchestrate autoreactive germinal center development in autoimmune BXD2 mice. *Nat. Immunol.* 9:166–175.
- Vinuesa, C.G., and C.C. Goodnow. 2004. Illuminating autoimmune regulators through controlled variation of the mouse genome sequence. *Immunity.* 20:669–679.
- Dent, A.L., A.L. Shaffer, X. Yu, D. Allman, and L.M. Staudt. 1997. Control of inflammation, cytokine expression, and germinal center formation by BCL-6. *Science.* 276:589–592.
- Ye, B.H., G. Cattoretti, Q. Shen, J. Zhang, N. Hawe, R. de Waard, C. Leung, M. Nouri-Shirazi, A. Orazi, R.S. Chaganti, et al. 1997. The BCL-6 proto-oncogene controls germinal-center formation and Th2-type inflammation. *Nat. Genet.* 16:161–170.
- Shaffer, A.L., X. Yu, Y. He, J. Boldrick, E.P. Chan, and L.M. Staudt. 2000. BCL-6 represses genes that function in lymphocyte differentiation, inflammation, and cell cycle control. *Immunity.* 13:199–212.
- Yu, D., A.H. Tan, X. Hu, V. Athanasopoulos, N. Simpson, D.G. Silva, A. Hutloff, K.M. Giles, P.J. Leedman, K.P. Lam, et al. 2007. Roquin represses autoimmunity by limiting inducible T-cell co-stimulator messenger RNA. *Nature.* 450:299–303.
- Linterman, M.A., R.J. Rigby, R. Wong, D. Silva, D. Withers, G. Anderson, N.K. Verma, R. Brink, A. Hutloff, C.C. Goodnow, and C.G. Vinuesa. 2009. Roquin differentiates the specialized functions of duplicated T cell co-stimulatory receptor genes *Cd28* and *Icos*. *Immunity.* In press.
- Haynes, N.M., C.D. Allen, R. Lesley, K.M. Ansel, N. Killeen, and J.G. Cyster. 2007. Role of CXCR5 and CCR7 in follicular Th cell positioning and appearance of a programmed cell death gene-1-high germinal center-associated subpopulation. *J. Immunol.* 179:5099–5108.
- Seo, S.J., M.L. Fields, J.L. Buckler, A.J. Reed, L. Mandik-Nayak, S.A. Nish, R.J. Noelle, L.A. Turka, F.D. Finkelman, A.J. Caton, and J. Erikson. 2002. The impact of T helper and T regulatory cells on the regulation of anti-double-stranded DNA B cells. *Immunity.* 16:535–546.
- Stockinger, B., and M. Veldhoen. 2007. Differentiation and function of Th17 T cells. *Curr. Opin. Immunol.* 19:281–286.
- Vogelzang, A., H.M. McGuire, D. Yu, J. Sprent, C.R. Mackay, and C. King. 2008. A fundamental role for interleukin-21 in the generation of T follicular helper cells. *Immunity.* 29:127–137.
- Nurieva, R.I., Y. Chung, D. Hwang, X.O. Yang, H.S. Kang, L. Ma, Y.H. Wang, S.S. Watowich, A.M. Jetten, Q. Tian, and C. Dong.

2008. Generation of T follicular helper cells is mediated by interleukin-21 but independent of T helper 1, 2, or 17 cell lineages. *Immunity*. 29:138–149.
35. Crotty, S., E.N. Kersh, J. Cannons, P.L. Schwartzberg, and R. Ahmed. 2003. SAP is required for generating long-term humoral immunity. *Nature*. 421:282–287.
36. Hron, J.D., L. Caplan, A.J. Gerth, P.L. Schwartzberg, and S.L. Peng. 2004. SH2D1A regulates T-dependent humoral autoimmunity. *J. Exp. Med.* 200:261–266.
37. Cannons, J.L., L.J. Yu, D. Jankovic, S. Crotty, R. Horai, M. Kirby, S. Anderson, A.W. Cheever, A. Sher, and P.L. Schwartzberg. 2006. SAP regulates T cell-mediated help for humoral immunity by a mechanism distinct from cytokine regulation. *J. Exp. Med.* 203:1551–1565.
38. McCausland, M.M., I. Yusuf, H. Tran, N. Ono, Y. Yanagi, and S. Crotty. 2007. SAP regulation of follicular helper CD4 T cell development and humoral immunity is independent of SLAM and Fyn kinase. *J. Immunol.* 178:817–828.
39. Veillette, A., S. Zhang, X. Shi, Z. Dong, D. Davidson, and M.C. Zhong. 2008. SAP expression in T cells, not in B cells, is required for humoral immunity. *Proc. Natl. Acad. Sci. USA*. 105:1273–1278.
40. Morra, M., R.A. Barrington, A.C. Abadia-Molina, S. Okamoto, A. Julien, C. Gullo, A. Kalsy, M.J. Edwards, G. Chen, R. Spolski, et al. 2005. Defective B cell responses in the absence of SH2D1A. *Proc. Natl. Acad. Sci. USA*. 102:4819–4823.
41. Paus, D., T.G. Phan, T.D. Chan, S. Gardam, A. Basten, and R. Brink. 2006. Antigen recognition strength regulates the choice between extrafollicular plasma cell and germinal center B cell differentiation. *J. Exp. Med.* 203:1081–1091.
42. Bossaller, L., J. Burger, R. Draeger, B. Grimbacher, R. Knoth, A. Plebani, A. Durandy, U. Baumann, M. Schlesier, A.A. Welcher, et al. 2006. ICOS deficiency is associated with a severe reduction of CXCR5+CD4 germinal center Th cells. *J. Immunol.* 177:4927–4932.
43. Akiba, H., K. Takeda, Y. Kojima, Y. Usui, N. Harada, T. Yamazaki, J. Ma, K. Tezuka, H. Yagita, and K. Okumura. 2005. The role of ICOS in the CXCR5+ follicular B helper T cell maintenance in vivo. *J. Immunol.* 175:2340–2348.
44. Ozaki, K., R. Spolski, C.G. Feng, C.F. Qi, J. Cheng, A. Sher, H.C. Morse 3rd, C. Liu, P.L. Schwartzberg, and W.J. Leonard. 2002. A critical role for IL-21 in regulating immunoglobulin production. *Science*. 298:1630–1634.
45. Munthe, L.A., A. Corthay, A. Os, M. Zangani, and B. Bogen. 2005. Systemic autoimmune disease caused by autoreactive B cells that receive chronic help from Ig V region-specific T cells. *J. Immunol.* 175:2391–2400.
46. Gray Parkin, K., R.P. Stephan, R.G. Apilado, D.A. Lill-Elghanian, K.P. Lee, B. Saha, and P.L. Witte. 2002. Expression of CD28 by bone marrow stromal cells and its involvement in B lymphopoiesis. *J. Immunol.* 169:2292–2302.
47. Delogu, A., A. Schebesta, Q. Sun, K. Aschenbrenner, T. Perlot, and M. Busslinger. 2006. Gene repression by Pax5 in B cells is essential for blood cell homeostasis and is reversed in plasma cells. *Immunity*. 24:269–281.
48. Krieg, A.M., and J. Vollmer. 2007. Toll-like receptors 7, 8, and 9: linking innate immunity to autoimmunity. *Immunol. Rev.* 220:251–269.
49. Vinuesa, C.G., M.C. Cook, M.P. Cooke, I.C. MacLennan, and C.C. Goodnow. 2002. Analysis of B cell memory formation using DNA microarrays. *Ann. NY Acad. Sci.* 975:33–45.
50. Griewank, K., C. Borowski, S. Rietdijk, N. Wang, A. Julien, D.G. Wei, A.A. Mamchak, C. Terhorst, and A. Bendelac. 2007. Homotypic interactions mediated by Slamf1 and Slamf6 receptors control NKT cell lineage development. *Immunity*. 27:751–762.
51. Nichols, K.E., J. Hom, S.Y. Gong, A. Ganguly, C.S. Ma, J.L. Cannons, S.G. Tangye, P.L. Schwartzberg, G.A. Koretzky, and P.L. Stein. 2005. Regulation of NKT cell development by SAP, the protein defective in XLP. *Nat. Med.* 11:340–345.
52. Komori, H., H. Furukawa, S. Mori, M.R. Ito, M. Terada, M.C. Zhang, N. Ishii, N. Sakuma, M. Nose, and M. Ono. 2006. A signal adaptor SLAM-associated protein regulates spontaneous autoimmunity and Fas-dependent lymphoproliferation in MRL-Fas<sup>lpr</sup> lupus mice. *J. Immunol.* 176:395–400.
53. Steinberg, A.D., J.B. Roths, E.D. Murphy, R.T. Steinberg, and E.S. Raveche. 1980. Effects of thymectomy or androgen administration upon the autoimmune disease of MRL/Mp-lpr/lpr mice. *J. Immunol.* 125:871–873.
54. Ettinger, R., S. Kuchen, and P.E. Lipsky. 2008. The role of IL-21 in regulating B-cell function in health and disease. *Immunol. Rev.* 223:60–86.
55. Odegard, J.M., B.R. Marks, L.D. Diplacido, A.C. Poholek, D.H. Kono, C. Dong, R.A. Flavell, and J. Craft. 2008. ICOS-dependent extrafollicular helper T cells elicit IgG production via IL-21 in systemic autoimmunity. *J. Exp. Med.* 205:2873–2886.
56. Ettinger, R., G.P. Sims, R. Robbins, D. Withers, R.T. Fischer, A.C. Grammer, S. Kuchen, and P.E. Lipsky. 2007. IL-21 and BAFF/BLyS synergize in stimulating plasma cell differentiation from a unique population of human splenic memory B cells. *J. Immunol.* 178:2872–2882.
57. Cappione, A., III, J.H. Anolik, A. Pugh-Bernard, J. Barnard, P. Dutcher, G. Silverman, and I. Sanz. 2005. Germinal center exclusion of autoreactive B cells is defective in human systemic lupus erythematosus. *J. Clin. Invest.* 115:3205–3216.
58. Grammer, A.C., R. Slota, R. Fischer, H. Gur, H. Girschick, C. Yarboro, G.G. Illei, and P.E. Lipsky. 2003. Abnormal germinal center reactions in systemic lupus erythematosus demonstrated by blockade of CD154-CD40 interactions. *J. Clin. Invest.* 112:1506–1520.
59. Goodnow, C.C., J. Sprent, B. Fazekas de St Groth, and C.G. Vinuesa. 2005. Cellular and genetic mechanisms of self tolerance and autoimmunity. *Nature*. 435:590–597.
60. Allen, C.D., T. Okada, and J.G. Cyster. 2007. Germinal-center organization and cellular dynamics. *Immunity*. 27:190–202.
61. Slingsby, J.H., P. Norsworthy, G. Pearce, A.K. Vaishnav, H. Issler, B.J. Morley, and M.J. Walport. 1996. Homozygous hereditary C1q deficiency and systemic lupus erythematosus. A new family and the molecular basis of C1q deficiency in three families. *Arthritis Rheum.* 39:663–670.
62. Hutloff, A., K. Buchner, K. Reiter, H.J. Baelde, M. Odendahl, A. Jacobi, T. Dorner, and R.A. Kroczeck. 2004. Involvement of inducible costimulator in the exaggerated memory B cell and plasma cell generation in systemic lupus erythematosus. *Arthritis Rheum.* 50:3211–3220.
63. Hutloff, A., A.M. Dittrich, K.C. Beier, B. Eljaschewitsch, R. Kraft, I. Anagnostopoulos, and R.A. Kroczeck. 1999. ICOS is an inducible T-cell co-stimulator structurally and functionally related to CD28. *Nature*. 397:263–266.
64. Rasheed, A.U., H.P. Rahn, F. Sallusto, M. Lipp, and G. Muller. 2006. Follicular B helper T cell activity is confined to CXCR5(hi)ICOS(hi) CD4 T cells and is independent of CD57 expression. *Eur. J. Immunol.* 36:1892–1903.
65. Phan, T.G., M. Amesbury, S. Gardam, J. Crosbie, J. Hasbold, P.D. Hodgkin, A. Basten, and R. Brink. 2003. B cell receptor-independent stimuli trigger immunoglobulin (Ig) class switch recombination and production of IgG autoantibodies by anergic self-reactive B cells. *J. Exp. Med.* 197:845–860.